A review of TiO$_2$ nanoparticles

GUPTA Shipra Mital[*] & TRIPATHI Manoj

University School of Basic and Applied Sciences, Guru Gobind Singh Indraprastha University, Sector 16C Dwarka, Delhi 110075, India

Climate change and the consumption of non-renewable resources are considered as the greatest problems facing humankind. Because of this, photocatalysis research has been rapidly expanding. TiO$_2$ nanoparticles have been extensively investigated for photocatalytic applications including the decomposition of organic compounds and production of H$_2$ as a fuel using solar energy. This article reviews the structure and electronic properties of TiO$_2$, compares TiO$_2$ with other common semiconductors used for photocatalytic applications and clarifies the advantages of using TiO$_2$ nanoparticles. TiO$_2$ is considered close to an ideal semiconductor for photocatalysis but possesses certain limitations such as poor absorption of visible radiation and rapid recombination of photogenerated electron/hole pairs. In this review article, various methods used to enhance the photocatalytic characteristics of TiO$_2$ including dye sensitization, doping, coupling and capping are discussed. Environmental and energy applications of TiO$_2$, including photocatalytic treatment of wastewater, pesticide degradation and water splitting to produce hydrogen have been summarized.

nanoparticles, photocatalyst, TiO$_2$, dye sensitization, doping, coupling, capping

1   Historical background

The growth of industry worldwide has tremendously increased the generation and accumulation of waste byproducts. In general, the production of useful products has been focused on and the generation of waste byproducts has been largely ignored. This has caused severe environmental problems that have become a major concern. Researchers all over the world have been working on various approaches to address this issue. Photoinduced processes have been studied and various applications have been developed. One important technique for removing industrial waste is the use of light energy (electromagnetic radiation) and particles sensitive to this energy to mineralize waste which aids in its removal from solution. Titanium dioxide (TiO$_2$) is considered very close to an ideal semiconductor for photocatalysis because of its high stability, low cost and safety toward both humans and the environment.

In 1964, Kato et al. [1] published their work on the photocatalytic oxidation of tetralin (1,2,3,4-tetrahydronaphthalene) by a TiO$_2$ suspension, which was followed by McLintock et al. [2] investigating the photocatalytic oxidation of ethylene and propylene in the presence of oxygen adsorbed on TiO$_2$. However, the most important discovery that extensively promoted the field of photocatalysis was the "Honda-Fujishima Effect" first described by Fujishima and Honda in 1972 [3]. This well-known chemical phenomenon involves electrolysis of water, which is related to photocatalysis. Photoirradiation of a TiO$_2$ (rutile) single crystal electrode immersed in an aqueous electrolyte solution induced the evolution of oxygen from the TiO$_2$ electrode and the evolution of hydrogen from a platinum counterelectrode when an anodic bias was applied to the TiO$_2$ working electrode. In 1977, Frank and Bard [4] examined the reduction of CN$^-$ in water using this technology. Schrauzer and Guth [5] reported the photocatalytic reduction of molecular nitrogen to ammonia and hydrazine over iron-doped TiO$_2$. Schrauzer et al. [6] also performed experiments with desert sand and minerals to reduce nitrogen.

*Corresponding author (email: shipra.mital@gmail.com)

In 1978, the first organic photosynthetic reaction was presented as an alternative photoinduced Kolbe reaction ($CH_3COOH \rightarrow CH_4 + CO_2$), which opened the field of photosynthetic reaction [7]. In 1983, Ollis and coworker [8] showed the extent of adsorption of several chlorinated hydrocarbons in terms of the Langmuir adsorption isotherm. In 1985, Matsunaga et al. [9] reported the photocatalytic activity of TiO_2 as a microbiocide effective at photokilling *Lactobacillus acidophilus*, *Saccharomyces cerevisiae* and *Escherichia coli*. In 1986, Fujishima et al. [10] used TiO_2 for photokilling tumor cells (HeLa cells). In 1991, O'Regan and Grätzel [11] reported an efficient solar cell containing nanosized TiO_2 particles coated with organic chromophore groups active under visible light. In 1995, Fujishima et al. [12] found that TiO_2 films coated with certain amount of silica acquired superhydrophilic properties after irradiation with UV light. In 1998, Wang et al. [13] developed highly hydrophilic TiO_2 surfaces with excellent anti-fogging and self-cleaning properties. In 2002, Watson et al. [14] used the sol-gel technique to coat magnetic particles with TiO_2, producing a novel magnetic photocatalyst that was easy to separate from a slurry-type photoreactor by application of an external magnetic field. In 2004, Sonawane et al. [15] reported Fe-doped TiO_2 films that could photodegrade up to 95% of methyl orange in a solution after exposure to sunlight for 3–4 h. In 2005, Sreethawong et al. [16] synthesized nanocrystalline mesoporous TiO_2 using sol-gel techniques combined with surfactant-assisted templating and evaluated its photocatalytic activity of the evolution of hydrogen from an aqueous methanol solution. In 2008, Diamandescu et al. [17] reported a hydrothermal synthesis of iron and europium codoped TiO_2 materials under mild conditions. The photocatalytic activity for the degradation of phenol was improved under both visible and UV light by codoping. In 2009, Lai and Lee [18] revealed the ability and mechanism of photoexcited TiO_2 nanoparticles modified with folic acid to kill cells. Folic acid was bound to TiO_2 nanoparticles to provide cell targeting specificity. These nanoparticles exhibited higher cytotoxicity under photoexcitation. Mizukoshi et al. [19] prepared rutile TiO_2 by anodic oxidation in a sulfuric acid electrolyte. Sulfur doping played an important role in the response of the product to visible light by narrowing the band gap of TiO_2, allowing the photocatalyst to effectively bleach an aqueous solution of methylene blue under irradiation with visible light of >413 nm. Wang et al. [20] synthesized TiO_2-coated magnetic silica that showed enhanced photocatalytic activity for the degradation of reactive brilliant red X-3B compared with Degussa P25 under both UV and visible light irradiation. Furthermore, the prepared composite photocatalyst had tunable magnetic properties.

Kaeugun et al. [21] synthesized polymorphic TiO_2 particles that were active under visible light using a water-based sol process followed by a solvent-based sol process with N-methylpyrrolidone as the solvent, all performed under ambient conditions. The photocatalytic activity under visible light was approximately 3.3 times higher than that of commercial TiO_2 (Kronos VLP7000).

Rocha et al. [22] carried out oil sludge treatment using heterogeneous photocatalysis (H_2O_2/UV/TiO_2) by applying black and white light reactors. Heterogeneous photocatalysis provided efficient degradation and mineralization of a large part of the organic matter in the oil sludge. It proved to be an alternative treatment for removing polyaromatic hydrocarbons (PAHs) from oil sludge, eliminating 100% of the PAH content from the oil sludge sample after 96 h of UV irradiation.

A significant amount of research on TiO_2 has been performed over the last five decades and a number of reviews on various aspects of TiO_2 have been published [12,23–28] to understand and summarize the progress in this field. In the present review, the properties of TiO_2 that make it suitable to act as a photocatalyst and various methods including dye sensitization, doping, coupling and capping that are used to improve its efficiency are discussed. Environmental and energy applications, including photocatalytic treatment of wastewater, pesticide degradation and water splitting by TiO_2 to produce hydrogen are summarized.

2   Chemical structure of TiO_2

TiO_2 belongs to the family of transition metal oxides. There are four commonly known polymorphs of TiO_2 found in nature: anatase (tetragonal), brookite (orthorhombic), rutile (tetragonal), and TiO_2 (B) (monoclinic) [23]. Besides these polymorphs, two additional high-pressure forms have been synthesized from the rutile phase. These are TiO_2 (II) [29] with a PbO_2 structure and TiO_2 (H) [30] with a hollandite structure. In this review, only the crystal structures (Table 1) [31–33] and properties of the rutile, anatase and brookite polymorphs are considered.

Rutile: Rutile TiO_2 has a tetragonal structure and contains 6 atoms per unit cell (Figure 1). The TiO_6 octahedron

Table 1   Crystal structure data for TiO_2 [31–33]

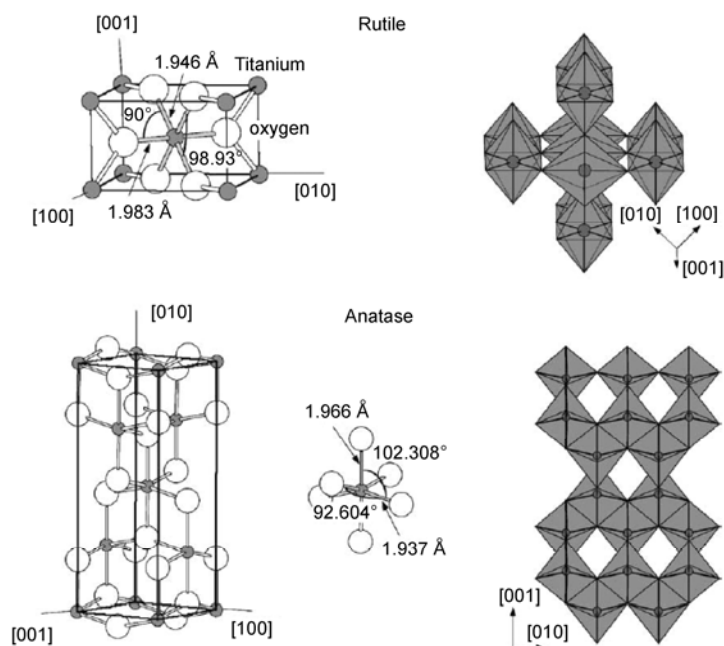| Properties	Rutile	Anatase	Brookite
Crystal structure	Tetragonal	Tetragonal	Orthorhombic
Lattice constant (Å)	$a = 4.5936$ $c = 2.9587$	$a = 3.784$ $c = 9.515$	$a = 9.184$ $b = 5.447$ $c = 5.154$
Space group	$P4_2/mnm$	$I4_1/amd$	Pbca
Molecule (cell)	2	2	4
Volume/ molecule (Å^3)	31.2160	34.061	32.172
Density (g cm^{-3})	4.13	3.79	3.99
Ti–O bond length (Å)	1.949 (4) 1.980 (2)	1.937(4) 1.965(2)	1.87–2.04
O–Ti–O bond angle	81.2° 90.0°	77.7° 92.6°	77.0°–105°

Figure 1   Crystal structures of the rutile and anatase phases of TiO$_2$ [27].

is slightly distorted [25–27]. The rutile phase is stable at most temperatures and pressures up to 60 kbar, where TiO$_2$ (II) becomes the thermodynamically favorable phase [34]. Zhang et al. [35] found that anatase and brookite structures transformed to the rutile phase after reaching a certain particle size, with the rutile phase becoming more stable than anatase for particle sizes greater than 14 nm. Once the rutile phase formed, it grew much faster than the anatase. The activity of the rutile phase as a photocatalyst is generally very poor. However, Sclafani et al [36]. concluded that the rutile phase can be active or inactive, depending on its preparation conditions.

Anatase: Anatase TiO$_2$ also has a tetragonal structure but the distortion of the TiO$_6$ octahedron is slightly larger for the anatase phase [28,33], as depicted in Figure 1. Muscat et al. [37] found that the anatase phase is more stable than the rutile at 0 K, but the energy difference between these two phases is small (~2 to 10 kJ/mol). The anatase structure is preferred over other polymorphs for solar cell applications because of its higher electron mobility, low dielectric constant and lower density [23]. The increased photoreactivity is because of the slightly higher Fermi level, lower capacity to adsorb oxygen and higher degree of hydroxylation in the anatase phase [38]. Selloni [39] reported that the reactivity of (001) facets is greater than that of (101) facets in an anatase crystal. Yang et al. [40] synthesized uniform anatase crystals containing 47% (001) facets using hydrofluoric acid as a morphology controlling agent.

Brookite: Brookite TiO$_2$ belongs to the orthorhombic crystal system. Its unit cell is composed of 8 formula units of TiO$_2$ and is formed by edge-sharing TiO$_6$ octahedra (Figure 2). It is more complicated, has a larger cell volume
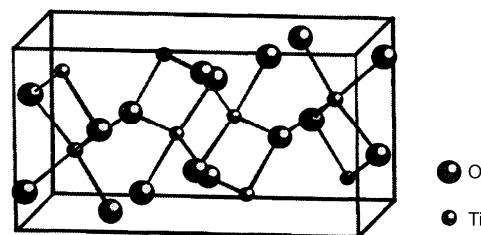

Figure 2   Lattice structure of brookite TiO$_2$ [33].

and is also the least dense of the 3 forms and is not often used for experimental investigations [26].

TiO$_2$ is a large band semiconductor, with band gaps of 3.2, 3.02, and 2.96 eV for the anatase, rutile and brookite phases, respectively [41]. The valence band of TiO$_2$ is composed of the 2p orbitals of oxygen hybridized with the 3d orbitals of titanium, while the conduction band is only the 3d orbitals of titanium [42]. When TiO$_2$ is exposed to near-UV light, electrons in the valence band are excited to the conduction band leaving behind holes (h$^+$), as shown in Figure 3. The excited electrons (e$^-$) in the conduction band are now in a purely 3d state and because of dissimilar parity, the transition probability of e$^-$ to the valence band decreases, leading to a reduction in the probability of e$^-$/h$^+$ recombination [43]. Anatase TiO$_2$ is considered to be the active photocatalytic component based on charge carrier dynamics, chemical properties and the activity of photocatalytic degradation of organic compounds. It has inherent surface band bending that forms spontaneously in a deeper region with a steeper potential compared with the rutile phase (Figure 4) [44] thus surface hole trapping dominates
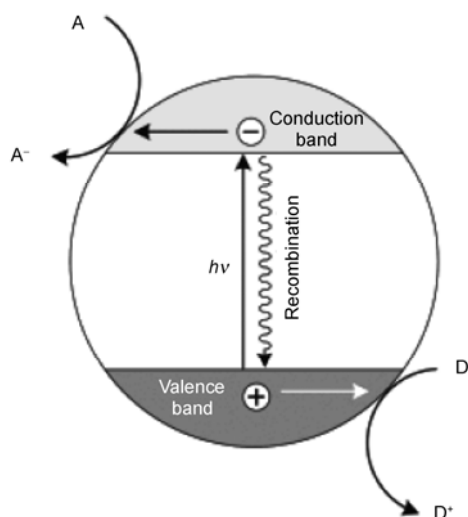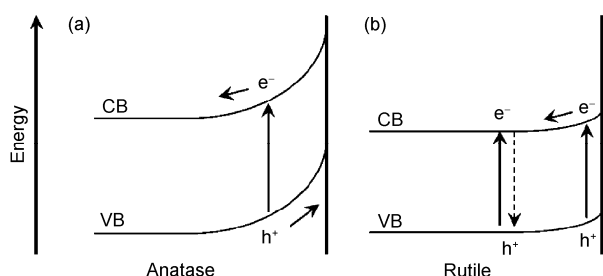
Figure 3   Mechanism of light absorption by TiO$_2$ [72].

Figure 4   Surface band bending of the anatase (a) and rutile phases of TiO$_2$ (b) [44].

because spatial charge separation is achieved by the transfer of photogenerated holes towards the surface of the particle *via* the strong upward band bending. However, in the rutile phase, the bulk recombination of electrons and holes occurs, so only holes very close to the surface are trapped and transferred to the surface.

3   Heat treatment of TiO$_2$

Heat treatment has a vital role in the synthesis of particles, affecting morphology, crystallinity and porosity, and causing a decline in surface area, loss of surface hydroxyl groups and inducing phase transformation. At high temperatures, (400°C and above) the removal of organic materials takes place. The surface area of TiO$_2$ decreases with calcination time and heating rate because of the collapse of pores in the TiO$_2$ powder caused by the transformation of amorphous TiO$_2$ to the anatase phase. Slow heating rates provide relatively mild conditions for phase transformation [45]. Hu et al. [46] have reported that TiO$_2$ normally undergoes an anatase-to-rutile phase transformation in the range from 600–700°C. The transformation was also affected by factors such as preparation conditions, precursors, impurities, oxygen vacancies and the primary particle size of the anatase phase.

Wang et al. [47] investigated the relationship between the phase transformation and photocatalytic activity of nanosized anatase powder and found that the highest photocatalytic activity for the degradation of acid red B under irradiation with visible light occurred when the rutile phase was on the point of appearing. TiO$_2$ containing both the rutile and anatase phases enhanced the effect of absorbed visible light than either of the pure phases. Once the rutile phase TiO$_2$ formed separately, the photocatalytic activity began to decrease rapidly. Ohtani et al. [48] proposed that TiO$_2$ with high photocatalytic activity could be achieved by fulfilling two requirements, namely, a large surface area for absorbing substrates and high crystallinity to reduce the rate of photoexcited e$^-$/h$^+$ recombination. Crystallinity increases and the surface area decreases with calcination temperature. The two requirements are partially satisfied at a moderate calcination temperature. Photocatalytic activity per unit mass of TiO$_2$ bulk reached a broad maximum at a calcination temperature of around 400°C. Yu et al. [49] showed that the duration of heat treatment also affected the photocatalytic activity of TiO$_2$ films. When TiO$_2$ films were heat-treated at 500°C, the rate constant first increased as the heat treatment time lengthened, reached a maximum after 60 min and then decreased upon further heat treatment.

4   TiO$_2$ nanoparticles

Various investigations have established that TiO$_2$ is much more effective as a photocatalyst in the form of nanoparticles than in bulk powder [50]. When the diameter of the crystallites of a semiconductor particle falls below a critical radius of about 10 nm, each charge carrier appears to behave quantum mechanically [11] as a simple particle in a box (Figure 5). As a result of this confinement, the band gap increases and the band edges shift to yield larger redox potentials [51]. However, the solvent reorganization free energy for charge transfer to a substrate remains unchanged. Because of the increased driving force and the unchanged solvent reorganization free energy, the rate constant of charge transfer in the normal Marcus region increases [52]. Using size-quantized semiconductor particles increases the photoefficiency of systems in which the rate-limiting step is charge transfer. Mill and Le Hunte [53] reported that because the absorption edge blue shifts with decreasing particle size, the redox potentials of the photogenerated electrons and holes in quantized semiconductor particles increased. In other words, quantized particles show higher photoactivity than macrocrystalline semiconductor particles.

Recently, TiO$_2$ has been prepared in the form of powders, crystals, thin films, nanotubes and nanorods. Liquid
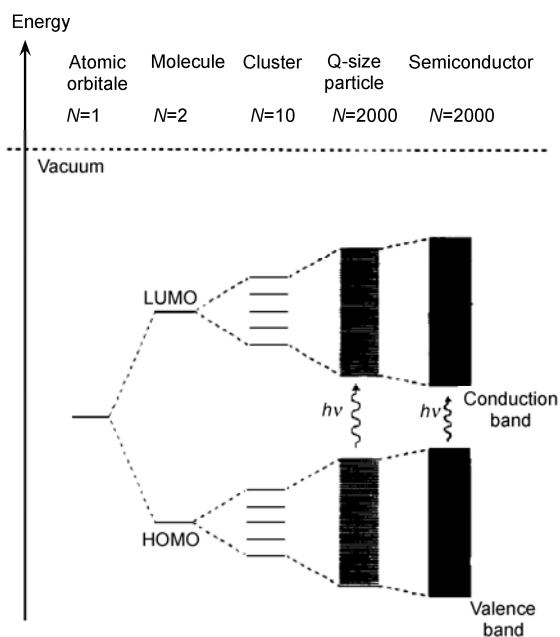
Figure 5 Molecular orbital model for particle growth of N monomeric units. The spacing of the energy levels (*i.e.*, density of states) varies among systems [51].

phase processing is one of the most convenient and commonly used methods in chemical synthesis. This method provides the advantages of controlling the stoichiometry, homogeneous products and allowing the formation of complex shapes and preparation of composite materials. However, some disadvantages exist including expensive precursors, long processing times, and the presence of carbon as an impurity. Dawson et al. [54] subjected mixed phase TiO_2 powders with different compositions and particle sizes to hydrothermal reaction with NaOH. The anatase phase component of the starting material was easily converted to trititanate nanotubes at 140°C. At 170°C, the rutile phase reacted to form trititanate plates and belts. When the reaction time was increased to 7 d, all of the TiO_2 was converted to trititanate and the morphology of the resulting product was exclusively nanoplates and belts, with no nanotubes. Yana et al. [55] synthesized pure rutile nanotubes by a hydrothermal process in NaOH water-ethanol solution starting from rutile-anatase TiO_2 particles. The nanotubes were up to several micrometers in length and had diameters of less than 20 nm. The type of alcohol and the ratio to water had a great impact on the morphology and structure of the final products. The rutile nanotubes exhibited different optoelectronic properties to those of the raw TiO_2. Mozia et al. [56] prepared modified titanate nanotubes (TNTs) *via* a hydrothermal method and focused on their application for the decomposition of Acid Red 18 (AR18) in water. Post-treatment calcination of the TNTs was carried out at temperatures of 400–700°C. The photocatalytic experiments revealed that the most active sample towards the decompo-

sition of AR18 was TNTs calcined at 600°C. However, the photocatalytic activity of the calcined titanate nanotubes, was lower than that of P25 regardless of the annealing temperature. Among the products and byproducts of AR18 photodegradation, organic acids (formic, acetic and oxalic) and inorganic ions (nitrite, nitrate, ammonia and sulfate) were detected.

Pradhan et al. [57] grew TiO_2 nanorods on a Tungsten carbide-Cobalt (WC–Co) substrate by metal-organic chemical vapor deposition. The diameter and length of the nanorods were about 50–100 nm and 0.5–2 mm, respectively. Nanorod growth was observed at 500°C, while most particles were deposited at 600°C and a thin coating was formed at 400°C. Limmer et al. [58] used sol electrophoretic deposition for template-based growth of TiO_2 nanorods. Uniform nanorods of approximately 45–200 nm in diameter and 10–60 μm in length were grown over large areas with almost unidirectional alignment. Attar et al. [59] fabricated aligned anatase and rutile TiO_2 nanorods and nanotubes with diameters of about 80–130 nm.

5 TiO_2 *vs.* other materials as a photocatalyst

The primary criteria for an efficient semiconductor photocatalyst is that the redox potential of the charge couple, *i.e.*, e^-/h^+, lies within the band gap domain of the photocatalyst. The energy level at the bottom of conduction band determines the reducing ability of photoelectrons while the energy level at the top of valence band determines the oxidizing ability of photogenerated holes [23].

The lower edge of the conduction band, upper edge of the valence band, and band gap of some of these sensitizers, as well as the standard potentials of several redox couples, are presented in Figure 6 [60]. The ordinate represents the internal energy not the free energy. The free energy of an e^-/h^+ pair is smaller than the band gap energy because e^-/h^+ pairs have a significant configurational entropy arising from the large number of translational states accessible to the mobile carriers in the conduction and valence bands.

Apart from possessing a suitable band gap energy, an ideal semiconductor should also be easy to produce and use, cost effective, photostable, nonhazardous for humans and the environment, effectively activated by solar light and able to catalyze the reaction effectively [23]. Most of the reported photocatalysts possess limitations, e.g., GaAs, PbS, and CdS are not sufficiently stable for catalysis in aqueous media as they readily undergo photocorrosion and are also toxic [53]. ZnO is unstable because it readily dissolves in water [61] to yield $Zn(OH)_2$ on the ZnO particle surface, which inactivates the catalyst over time. Fe_2O_3, SnO_2, and WO_3 possess a conduction band edge at an energy level below the reversible hydrogen potential, thus systems using these materials require application of an external electrical bias to complete the water splitting reaction and achieve
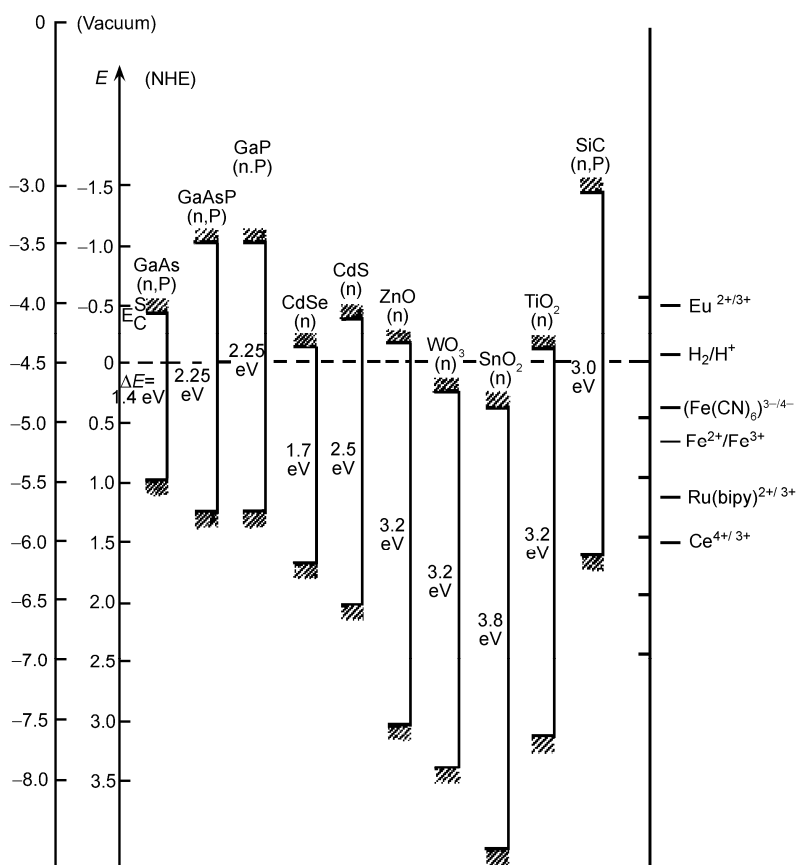
Figure 6 Band positions of several semiconductors in contact with an aqueous electrolyte at pH 1 [60].

hydrogen evolution at the cathode [62].

TiO$_2$ is close to being an ideal photocatalyst and the benchmark for photocatalysis performance. TiO$_2$ is cheap, photostable in solution and nontoxic. Its holes are strongly oxidizing and redox selective. For these reasons, several novel heterogeneous photocatalytic reactions have been reported at the interface of illuminated TiO$_2$ photocatalyst, and TiO$_2$-based photocatalysis has been researched exhaustively for environmental cleanup applications. The single drawback is that it does not absorb visible light [23]. To overcome this problem, several approaches including dye sensitization, doping, coupling and capping of TiO$_2$ have been studied extensively. An overview of these approaches is presented in the following sections.

6 Dye sensitization

Surface sensitization of a wide band gap semiconductor photocatalyst such as TiO$_2$ *via* chemisorbed or physisorbed dyes can increase the efficiency of the excitation process and expand the wavelength range of excitation for the photocatalyst. This occurs through excitation of the sensitizer followed by charge transfer to the semiconductor.

Charge carriers can form in semiconductor particles by exciting a dye attached to the surface of the photocatalyst. The excited state can inject either a hole, or more commonly, an electron to the particle. Highly efficient charge injection is observed when a monolayer of a dye is dispersed on a photocatalyst with a high surface area. This sensitization increases the range of wavelength response of the photocatalyst, which is very important for photocatalyst to operate under natural sunlight. Photosensitization of semiconductors by various dyes has been monitored by nanosecond and picosecond flash photolysis as well as femtosecond spectroscopy. The electron injection and back electron-transfer rates from the dye to the photocatalyst depend upon the nature of the dye molecules, properties of the TiO$_2$ nanoparticles and the interactions between the dye and nanoparticles [63].

Nishikiori et al. [64] found that an increase in the overall crystallinity of TiO$_2$ nanoparticles increased the surface quality of the nanoparticles, which improved the anchoring geometry of the dye on their surfaces and led to faster electron injection. However, back electron transfer *via* recombination with oxidized dye molecules, which decreases the quantum yield of photon-to-current conversion, was also enhanced as the crystallinity of the TiO$_2$ nanoparticles was

increased. Amorphous TiO_2 containing some alkoxide groups causing defects inside and outside the amorphous particle-like units served as trapping states with long lifetimes for electrons injected from the excited dye molecules, giving a relatively slow recombination rate. After increasing the crystallinity of the TiO_2 particles, the trapping states were mostly eliminated [65] and surface states formed that increased the rate of back electron transfer to the oxidized dye.

Li et al. [66] reported efficient photocatalytic decomposition of 2,4-dichlorophenol (2,4-DCP) under visible light irradiation by TiO_2 using xanthene dye as a sensitizer. The efficiency of decomposition of 2,4-DCP by TiO_2 sensitized with various dyes decreased in the following order: eosin Y ≈ rose bengal > erythrosine > rhodamine B.

Dye-sensitized TiO_2 has received much attention in photovoltaic applications, such as dye-sensitized cells [11] and photolysis of water to generate hydrogen [67]. TiO_2 is a preferred semiconductor for dye-sensitized solar cells because it is a stable photoelectrode in photoelectrochemical cells even under extreme conditions. Its conduction band edge lies slightly below the excited state energy level of many dyes, which is one condition required for efficient electron injection. Its high dielectric constant provides effective electrostatic shielding of the injected electron from the oxidized dye molecule, thus preventing its recombination before reduction of the dye by the redox electrolyte. The high refractive index of TiO_2 results in efficient diffuse scattering of the light inside the porous photoelectrode, which significantly enhances light absorption [68]. Grätzel developed a highly porous TiO_2 substrate electrode called a "Grätzel cell" containing a dye (e.g., tris(bipyridyl) ruthenium, coumarin) as a sensitizer [11]. Such cells are a cheap alternative to amorphous silicon solar cells. However, very few dyes are stable towards photodegradation and can provide a high photocurrent quantum yield [69].

When sensitized by dyes, TiO_2 catalysts can make full use of visible light to realize photocatalytic reactions. However, dyes themselves can undergo photodegradation or form intermediates that need to be disposed of ulteriorly [70].

7   Doping

Doping of TiO_2 has been an important approach in band gap engineering to change the optical response of semiconductor photocatalysts. The main objective of doping is to induce a bathochromic shift, *i.e.*, a decrease of the band gap or introduction of intra-band gap states, which results in the absorption of more visible light. Doping may lead to photocatalytic systems that exhibit enhanced efficiency [23]. It is desirable to maintain the integrity of the crystal structure of the photocatalyst while changing its electronic structure by doping. It is easier to replace Ti^{4+} in TiO_2 with a cation than

to substitute O^{2-} with another anion because of the difference in the charge states and ionic radii [24]. Nanomaterials show a higher tolerance to structural distortion than bulk materials due to their inherent lattice strain. As a result, the surface modification of TiO_2 nanoparticles appears to be more beneficial than the modification of bulk TiO_2 [71].

7.1   Doping with transition metal cations

Transition metal ions can provide additional energy levels within the band gap of a semiconductor. Electron transfer from one of these levels to the conduction band requires lower photon energy than in the situation of an unmodified semiconductor. TiO_2 has been doped with many different transition metals [72–86]. Grätzel et al. [73] studied the effect of doping TiO_2 with transition metals such as Fe, V, and Mo by electron paramagnetic resonance. Choi et al. [74] carried out a systematic investigation of the photoreactivity of TiO_2 doped with 21 different metal ions. Dopants such as Fe(III), Mo(V), Ru(III), Os(III), Re(V) and V(V) substantially enhanced the photochemical reactivity of TiO_2 for the oxidation of $CHCl_3$ and reduction of CCl_4.

Enhancing the rate of photoreduction by doping a semiconductor with metal ions can produce a photocatalyst with an improved trapping-to-recombination rate ratio. However, when metal ions or oxides are incorporated into TiO_2 by doping, the impurity energy levels formed in the band gap of TiO_2 can also lead to an increase in the rate of recombination between photogenerated electrons and holes. Photocatalytic reactions can only occur if the trapped electron and hole are transferred to the surface of the photocatalyst. This means that metal ions should be doped near the surface of the photocatalyst to allow efficient charge transfer. In the case of doping at a high concentration, metal ions can behave as recombination centers. Joshi et al. [75] reported the adverse effect of doping TiO_2 with transition metal ions on photocatalytic activity because of the formation of localized d-states in the band gap of TiO_2. Localized d-states act as trapping sites that capture electrons from the conduction band or holes from the valence band.

From a chemical point of view, TiO_2 doping is equivalent to the introduction of defect sites like Ti^{3+} into the semiconductor lattice, where the oxidation of Ti^{3+} species is kinetically fast compared with the oxidation of Ti^{4+}. The differences in photoactivity derive from the change in the diffusion length of the minority carriers [76]. For optimal e^-/h^+ separation, the magnitude of the potential drop across the space-charge layer should not fall below 0.2 V [77]. The dopant content directly influences the rate of e^-/h^+ recombination by the equation: $W = (2\ \varepsilon\varepsilon_o V_s/eN_d)$, where W is the thickness of the space-charge layer, ε is the static dielectric constant of the semiconductor, ε_o is the static dielectric constant in a vacuum, V_s is the surface potential, N_d is the number of dopant donor atoms, and e is the electron charge [78]. As the concentration of the dopant increases, the

space-charge region becomes narrower and the electron-hole pairs within the region are efficiently separated by the large electric field before recombination. However, when the concentration of doping is high, the space-charge region is very narrow so the penetration depth of light into TiO_2 greatly exceeds the width of the space-charge layer. Therefore, the rate of recombination of photogenerated electron-hole pairs in the semiconductor increases because there is no driving force to separate them. Consequently, there is an optimum concentration of dopant ions where the thickness of the space-charge layer is similar to the depth of light penetration. Xin et al. [79] reported enhanced photocatalytic activity of TiO_2 containing a low doping concentration of Fe^{3+} (Fe/Ti ≤ 0.03 mol) and reduced photocatalytic activity at higher concentrations. Li et al. [80] prepared zero-valent Fe-doped TiO_2 nanorods by an *in situ* reduction route using templareTiO_2 nanorods that were pre-synth- esized using a traditional alkaline hydrothermal method. The photocatalytic degradation of acetic acid and formaldehyde by the doped nanorods was investigated under irradiation with UV light. The photoactivity of the Fe-doped TiO_2 nanorods was much higher than that of Degussa P-25. Periyasami et al. [81] synthesized pure and Fe-doped nanocrystalline TiO_2 by combining a sol-gel technique with hydrothermal treatment. Doping with Fe caused a significant shift in absorption towards the visible region compared with that of Degussa P-25 and pure TiO_2. The photocatalytic activity of TiO_2 doped with Fe exceeded those of undoped commercial and synthesized pure TiO_2 for the oxidative degradation of 2,4,6-trichlorophenol.

Khan et al. [82] synthesized TiO_2 nanotubes hydrothermally and doped them with ruthenium using an ion exchange method. The resulting photocatalyst was active under visible light, exhibiting higher photocatalytic activity (>80%) for the degradation of methylene blue than undoped nanotubes. The loading method, size of ruthenium particles and metal dispersion pattern at the surfaces of the nanotubes had a great influence on their photocatalytic performance. Prasad et al. [83] studied modified TiO_2 nanotubes as powder decontaminant for sulfur mustard, a deadly chemical warfare agent. Decontamination reactions were carried out at room temperature. Hydrolysis of sulfur mustard was accelerated on Ag^+-doped TiO_2 nanotubes compared with Cu^{2+}, Ni^{2+}, Co^{2+}, Mn^{2+} and Ru^{3+}-doped TiO_2 nanotubes. Thiodiglycol and 1,4-oxathiane were observed to be the major products formed except for on the Ru^{3+}-doped TiO_2 nanotubes, where sulfur mustard sulfoxide was formed.

El-Bahy et al. [84] synthesized TiO_2 nanoparticles doped with lanthanide ions (La^{3+}, Nd^{3+}, Sm^{3+}, Eu^{3+}, Gd^{3+} and Yb^{3+}) by a sol-gel method. Gd^{3+}-doped TiO_2 had the lowest band gap, smallest particle size and the highest surface area and pore volume of the samples. The dopant lanthanide ions enhanced the photocatalytic activity of TiO_2 to some extent compared with pure TiO_2 and Gd^{3+}-doped TiO_2 was the most effective photocatalyst. Wang et al. [85] prepared

Gd-doped TiO_2 hollow spheres were using hydrothermally prepared carbon spheres as a template. The photocatalytic activity of the as-prepared hollow TiO_2 spheres was determined from their degradation of the dye Reactive Brilliant Red under irradiation with visible light. A Gd doping content of 4% provided optimal photocatalytic activity for the degradation of Reactive Brilliant Red. They also synthesized Ce-doped TiO_2 hollow spheres using carbon spheres as a template and Ce-doped TiO_2 nanoparticles as building blocks [86]. The rate constant for the degradation of the dye X-3B at with a Ce doping content of 4% was almost 31 times higher than that of Degussa P25.

7.2 Addition of noble metals

Addition of noble metals is another approach for the modifying photocatalysts. Noble metals including Pt, Ag, Au, Pd, Ni, Rh and Cu have been reported to be very effective at enhancing photocatalysis by TiO_2 [87–92]. Because the Fermi levels of these noble metals are lower than that of TiO_2, photoexcited electrons can be transferred from the conduction band of TiO_2 to metal particles deposited on the surface of TiO_2, while photogenerated holes in the valence band remain on TiO_2. This greatly reduces the possibility of electron-hole recombination, resulting in efficient separation and higher photocatalytic activity. Numerous studies have found that the properties of these kinds of composites depend strongly on the size of the metal particle, dispersion and composition. When the size of the metal particles is less than 2.0 nm, the composites display exceptional catalytic behavior [93]. It has been suggested that too high a concentration of metal particles reduces photon absorption by TiO_2 and allows the metal particles to become electron-hole recombination centers, resulting in lower efficiency [94].

Rupa et al. [87] synthesized TiO_2 nanoparticles by the sol-gel technique and doped the nanoparticles with about 1% noble metal (M/TiO_2, M = Ag, Au, and Pt) through photodeposition. M/TiO_2 catalysts showed remarkable photocatalytic activity towards the decolorization of tartrazine even under visible irradiation. The order of the photocatalytic activity of the different catalysts was: Au/TiO_2 > Ag/TiO_2 ~ Pt/TiO_2 > Synthesized TiO_2 > TiO_2 (P-25 Degussa). Papp et al. [88] found that the addition of palladium to TiO_2 powder by either photodecomposition or thermal decomposition increased its photocatalytic activity towards the degradation of 1,4-dichlorobenzene. Thampi et al. [89] reported that Rh/TiO_2 samples exhibited a high activity for CO_2 photoreduction using hydrogen to selectively produce CH_4. Adachi et al. [90] reported CO_2 reduction using copper-doped TiO_2 powder at ambient temperature. The Cu-TiO_2 catalyst yielded, specifically, methane and ethylene. Wong et al. [91] observed that visible light induced H_2 production from an aqueous methanol solution over a Cu-ion doped TiO_2 photocatalyst. More recently, Wu and Lee [92] reported that deposition with Cu particles

greatly enhanced the photocatalytic activity of TiO_2 for producing H_2 from aqueous methanol solution.

7.3 Doping with metalloids

Xu et al. [95] prepared TiO_2 photocatalyst that was active under visible light by doping with boron using sodium borohydride at 55°C under hydrothermal conditions. Compared with pure TiO_2, the doped sample exhibited stronger absorption in the visible region and also showed a larger surface area. The photocatalytic activity was evaluated by measuring the degradation of Reactive Brilliant Red and 4-chlorophenol under irradiation with visible light. The photocatalytic activities of the samples showed the following order: B-doped TiO_2 (hydrothermal method) > B-doped TiO_2 (sol-gel method) > pure TiO_2 > Degussa P25. The same group also prepared B-doped TiO_2 hollow spheres [96] using hydrothermally prepared carbon spheres as a template. The photocatalytic activity of these TiO_2 spheres was determined by degrading Reactive Brilliant Red under visible light irradiation. It was revealed that the photocatalytic activity of the hollow TiO_2 spheres was almost 22 times greater than that of Degussa P25.

7.4 Doping with anions

Many studies have been devoted to the development of TiO_2 that is responsive to visible light by doping it with various anions [97–103] as a substitute for oxygen in the TiO_2 lattice. For these anion-doped TiO_2 photocatalysts, the mixing of the p states of the doped anion (N, S or C) with the O 2p states shifts the valence band edge upwards, narrowing the band gap energy of TiO_2. Unlike metal cations, anions are less likely to form recombination centers and therefore, are more effective at enhancing the photocatalytic activity of TiO_2 [104].

Asahi et al. [97] calculated the electronic band structures of TiO_2 containing different substitutional dopants including C, N, F, P and S. Substitutional doping with N narrowed the band gap most significantly because its p state mixed with the O 2p states. In addition, molecular dopants like NO and N_2 gave rise to bonding states below the O 2p valence band and antibonding states deep in the band gap (N_i and N_{i+s}) that were well screened and hardly interacted with the band states of TiO_2. Diwald et al. [98] incorporated nitrogen monoanions into single crystals of TiO_2 by sputtering with N_2^+/Ar^+ mixtures and subsequent annealing to 627°C under ultrahigh vacuum conditions. This modified catalyst exhibited an unexpected blue shift in the O_2 photodesorption compared with that of undoped crystals of TiO_2. Ao et al. [99] prepared N-doped TiO_2 hollow spheres by a one-pot hydrothermal method using urea as precursor of nitrogen. The photocatalytic activity of the spheres was determined by degrading Reactive Brilliant Red dye X-3B under irradiation with visible light and showed higher photocatalytic activity than undoped TiO_2 hollow spheres and commercial Degussa P25. Dong et al. [100] synthesized N-doped TiO_2 nanotube array by annealing anodized TiO_2 nanotubes with ammonia at 500°C. The array exhibited enhanced photocatalytic efficiency for the photocatalytic degradation of methyl orange under visible light irradiation compared with undoped nanotubes because nitrogen doping narrowed the band gap of the nanotubes.

Yu et al. [101] found that F-doped TiO_2 exhibited higher photocatalytic activity for the oxidation of acetone into CO_2 than undoped TiO_2. Various reports state that C-doped TiO_2 is also remarkably effective at catalyzing this reaction [102,103]. Sakthivel and Kisch [102] showed that C-doped TiO_2 was five times more active than N-doped TiO_2 toward the degradation of 4-chlorophenol by artificial light ($\lambda \geq$ 455 nm). Park et al. [103] reported that $TiO_{2-x}C_x$ nanotube arrays exhibit much higher photocurrent densities and more efficient water splitting under irradiation with visible light than pure TiO_2 nanotube arrays.

7.5 Codoping

Codoping of TiO_2 may be used as an effective way to improve charge separation. Yang et al. [105] reported that monocrystalline TiO_2 codoped with optimal concentrations of Eu^{3+} and Fe^{3+} (1% Fe^{3+} and 0.5% Eu^{3+}) showed significantly enhanced photocatalytic activity compared with undoped TiO_2. Fe^{3+} serves as a hole trap and Eu^{3+} as an electron trap, increasing the rates of anodic and the cathodic processes *via* improved interfacial charge transfer. Vasiliu et al. [106] reported that Fe- and Eu-doped TiO_2 showed a red shift in its absorption spectrum and high photoactivity for the degradation and catalytic oxidation reactions of styrene and phenol, respectively, when exposed to visible light.

Song et al. [107] prepared (Cu, N)-codoped TiO_2 nanoparticles and investigated the influence of the amounts of Cu and N codoped into TiO_2 on the photocatalytic activity. Codoping of TiO_2 with N and Cu extended absorption upto 590 nm and gave higher photocatalytic activity than pure N- or Cu-doped TiO_2 for the photocatalytic degradation of xylenol orange, thus revealing a potential application in degrading organic pollutants. Xu et al. [108] synthesized (Ce, C)-codoped TiO_2 using a modified sol-gel method under mild conditions. The photocatalytic activity of (Ce, C)-codoped TiO_2 for degradation of Reactive Brilliant Red X-3B under visible light was significantly improved compared with that of C-doped TiO_2, undoped TiO_2 and Degussa P25 because cerium doping slowed the radiative recombination of photogenerated electrons and holes in TiO_2. Shen et al. [109] prepared a (N, Ce)-codoped TiO_2 photocatalyst by the sol-gel route that could degrade nitrobenzene under irradiation with visible light. Nitrogen atoms were incorporated into the TiO_2 crystal structure and narrowed the band gap energy. The dopant cerium atoms existed in the form of Ce_2O_3, and were dispersed on the surface of

TiO$_2$. The improvement in the photocatalytic activity was ascribed to the synergistic effects of nitrogen and cerium codoping. Yang et al. [110] codoped TiO$_2$ with metallic silver and vanadium oxide using a one-step sol-gel solvothermal method in the presence of a triblock copolymer surfactant (P123). The resulting Ag/V-TiO$_2$ three-component junction system exhibited the highest photocatalytic activity for the degradation of rhodamine B and Coomassie Brilliant Blue G-250 under both visible and UV light exceeding that of Degussa P25, pure TiO$_2$, singly-doped TiO$_2$ (Ag/TiO$_2$ or V-TiO$_2$) as well as a P123-free-Ag/V-TiO$_2$ codoped system.

8 Coupled/composite TiO$_2$

It is possible to create coupled colloidal structures, in which illumination of one semiconductor produces a response in the other semiconductor at the interface between them [53]. Coupled semiconductor photocatalysts exhibit very high photocatalytic activity for both gas and liquid phase reactions by increasing the charge separation and extending the energy range of photoexcitation. The geometry of particles, surface texture, and particle size play a significant role in interparticle electron transfer. Appropriate placement of the individual semiconductors and optimal thickness of the covering semiconductor are crucial for efficient charge separation.

There has been much interest in coupling different semiconductor particles with TiO$_2$, with coupled samples such as TiO$_2$-CdS, Bi$_2$S$_3$-TiO$_2$, TiO$_2$-WO$_3$, TiO$_2$-SnO$_2$, TiO$_2$-MoO$_3$, and TiO$_2$-Fe$_2$O$_3$ being reported [111–118]. The coupled structure that has received the most attention is that consisting of CdS and TiO$_2$ colloidal particles. As illustrated in Figure 7, it is possible to irradiate CdS with light of lower energy than that needed to electronically excite TiO$_2$ particles, so the photogenerated electron can be injected from CdS to TiO$_2$ while hole remains in CdS [53]. The electron transfer from CdS to TiO$_2$ increases the charge separation
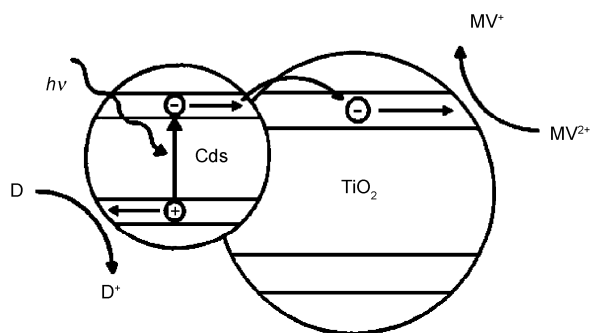

Figure 7 Schematic illustration of the photoinduced charge injection process that occurs upon excitation of the CdS component of a CdS/TiO$_2$ colloid in the presence of a sacrificial electron donor D and electron scavenger (methyl viologen, MV^{2+}) [53]

and the efficiency of the photocatalytic process. The separated electron and hole are then free to undergo electron transfer with adsorbates on the surface of the catalyst. Methyl viologen was almost completely reduced using coupled CdS/TiO$_2$ as a photocatalyst under irradiation with visible light [112].

Bi$_2$S$_3$ nanoparticles with a direct band gap of 1.28 eV are a good material for the photosensitization of nanocrystalline TiO$_2$. The conduction band of Bi$_2$S$_3$ nanoparticles is less anodic than the conduction band of TiO$_2$ and the valence band is more cathodic than the valence band of TiO$_2$ [113], enhancing electron injection from the excited state of Bi$_2$S$_3$ into TiO$_2$. Bessekhouad et al. [114] studied a Bi$_2$S$_3$/TiO$_2$ junction prepared by precipitation of different concentrations of Bi$_2$S$_3$ onto TiO$_2$. Bi$_2$S$_3$ absorbed a large portion of visible light and when the junction contained 10 wt% Bi$_2$S$_3$, the absorbance started at 800 nm.

The coupled system WO$_3$/TiO$_2$ has been used as a photocatalyst for decades. Both the upper edge of the valence band and the lower edge of the conduction band of WO$_3$ are lower than those of TiO$_2$, as illustrated in Figure 6. WO$_3$ can be excited by illumination with visible light and the photogenerated holes can transfer from WO$_3$ to TiO$_2$. Song et al. [115] observed that loading of WO$_3$ on the TiO$_2$ surface improved the decomposition of 1,4-dichlorobenzene in aqueous solution by up to 5.9 times compared with pure TiO$_2$. Because the standard reduction potential between W(VI) and W(V) is only –0.03 V, it was deduced that electrons in the conduction band of TiO$_2$ could be easily accepted by WO$_3$. The electrons in WO$_3$ would then be transferred to the oxygen molecules adsorbed on the surface of TiO$_2$. Grandcolas et al. [116] reported porogen template-assisted sol-gel synthesis of coupled rutile-anatase TiO$_2$ with a high surface area. It acted as a support for WO$_3$, which extended the absorption to the visible region and improved the photocatalytic performance. CO oxidation, diethylsulfide degradation and hydrogen production by this system were reported.

The coupled system SnO$_2$/TiO$_2$, where TiO$_2$ plays the role of photosensitizer for SnO$_2$, also attracts much interest. Pure SnO$_2$ shows little catalytic activity compared with TiO$_2$-based photocatalysts because the band gap of SnO$_2$ (3.5–3.8 eV) is not sufficient to initiate photocatalytic reactions, even after UV illumination. The work function and electron affinity of TiO$_2$ are both around 4.2 eV while the work function of SnO$_2$ is around 4.4 eV and its electron affinity is about 0.5 eV larger than that of TiO$_2$. The Fermi energy level of TiO$_2$ is higher than that of SnO$_2$ because of its smaller work function so electron transfer occurs from the conduction band of TiO$_2$ to the conduction band of SnO$_2$ and hole transfer occurs from the valence band of SnO$_2$ to the valence band of TiO$_2$ (Figure 8) [117]. Vinodgopal et al. [118] reported that the rate of photocatalytic degradation of several textile azo dyes increased by 10 times using an SnO$_2$/TiO$_2$ composite system as a result of improved charge
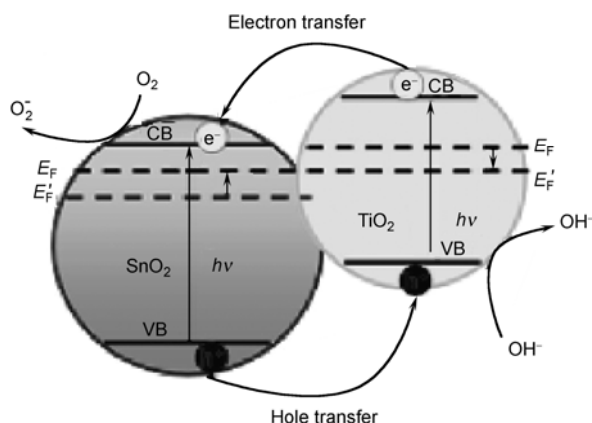
Figure 8   Schematic diagram showing the energy band structure and electron-hole pair separation in a SnO_2/TiO_2 heterostructure [117]

separation.

9   Hybridization

Conjugated materials are excellent candidates for improving the transportation of photocarriers in photocatalysis by forming electronic interactions with TiO_2 because of its unique electron and hole transport properties. Some efforts have been made to electronically combine conjugated materials with photocatalysts in recent years.

Zhang et al. [119] have demonstrated that surface hybridization of TiO_2 with a few molecular layers of graphite-like carbon yielded an efficient photocatalyst exhibiting photo-induced electrons with high mobility at the graphite-like carbon/TiO_2 interface because of the electronic interactions between the materials. In addition, the response of TiO_2 was extended into the visible range due to the electronic coupling of p states of the graphite-like carbon and conduction band states of TiO_2. TiO_2 with a carbon shell with a thickness of three molecular layers showed a photocatalytic activity that was twice as high as that of Degussa P25 TiO_2 under UV irradiation. Zhang et al. [120] also obtained an efficient TiO_2 photocatalyst by surface hybridization with a thin layer of C_{60} molecules. The photocatalytic performance of C_{60}-hybridized TiO_2 under UV irradiation was enhanced four times compared with that of a P25-TiO_2 photocatalyst. The increase in photocatalytic activity strongly depended on the coverage of C_{60} molecules on the surface of TiO_2.

Ji et al. [121] fabricated a TiO_2/hydroxyapatite composite granular photocatalyst with a novel microstructure from commercially available α-tri-calcium phosphate and TiO_2 powders using a process based on the liquid immiscibility effect followed by precalcination and hydrothermal treatment. A blue shift of the absorption edge of 16 nm was observed upon hybridization of TiO_2 and hydroxyapatite. Microstructure analysis indicated that the granule contained rod-shaped hydroxyapatite crystals with surfaces covered by nanosized TiO_2 particles. In the composite granules, the active anatase surface was retained effectively and they operated as three-dimensional, highly porous, size-controllable small reactors. Quantitative analysis of the decomposition of methylene blue as a target pollutant compound indicated that the photocatalytic reaction rate constant was greatly increased compared with that of bulk TiO_2.

Takeuchi et al. [122] prepared various Ti oxide-based photocatalysts such as highly dispersed Ti oxide species within zeolite frameworks, TiO_2 nanoparticles hybridized with hydrophobic zeolite adsorbents and TiO_2 thin films responsive to visible light. A high photocatalytic reactivity was observed for the photocatalytic decomposition of NO_x and the photocatalytic reduction of CO_2 with H_2O using the TiO_2 semiconducting photocatalysts.

10   Doped and coupled TiO_2

From the above discussion, it is clear that doping of TiO_2 can enhance its visible light activity significantly by changing the position of the conduction or valance bands by introducing impurity energy levels. The coupling of TiO_2 with other narrow band gap semiconductors could also enhance its visible light activity because electrons or holes photogenerated in the narrow band gap materials could be injected into TiO_2, resulting in better charge separation in the illuminated photocatalyst by enhancing the lifetimes of the e^- and h^+. To further improve the photocatalytic performance, various attempts have been made to study the combined effect of coupling and doping.

Zhang et al. [123] fabricated a photoelectrode photocatalyst that was active under visible light by modifying TiO_2 nanotubes with CdS and S^{6+}. S^{6+} doping narrowed the band gap to enhance the visible light response of TiO_2 and reduced the potential of the conduction band of TiO_2, accelerating the electron transfer between TiO_2 and CdS. The free energy (ΔG) for electron transfer between a donor and acceptor is a useful predictor of the activity of a coupled photocatalyst. ΔG for electron transfer between S-doped TiO_2 and CdS was determined according to the following equation [124]: $\Delta G = -F(E^0(S–TiO_2(x)) - E^0(CdS))$, where F is Faraday's constant (96486 C/mol), $E^0(CdS)$ and $E^0(S–TiO_2(x))$ are the standard reduction potentials of the conduction band electrons of CdS and $S–TiO_2(x)$, respectively, and "x" denotes the concentration of S^{6+}. Increasing the concentration of S^{6+} caused ΔG to decrease, suggesting that electron transfer between TiO_2 and CdS occurred more readily so the amount of carriers is increased, enhancing the photoactivity. Consequently, it was concluded that decreasing ΔG was one of the reasons for the high activity of $CdS/S–TiO_2(x)$. Thus, by such modification, a promising photocatalyst can be produced.

Kumar and Jain [125] investigated the effect of addition of metal ions on the photoactivity of CdS-TiO$_2$ composite photocatalysts. Doping either Cd(OH)$_2$-coated Q-CdS or TiO$_2$ with Ag$^+$ prior to their coupling (Ag$^+$-doped Cd(OH)$_2$-coated Q-CdS coupled with TiO$_2$ and Ag$^+$-doped TiO$_2$ coupled with Cd(OH)$_2$-coated Q-CdS) produced a three component composite catalyst [CdS-TiO$_2$-Ag$_2$S] system. The presence of Ag$^+$ in the TiO$_2$ lattice promoted the charge separation by scavenging shallowly trapped electrons from the conduction band of CdS and causing the trapped holes to move to deeper traps. The Ag-doped coupled photocatalyst system was found to be about twice as photocatalytically efficient as the undoped Q-CdS-TiO$_2$ composite for performing synthetic photochemistry.

11 Capping

The coating of one semiconductor or metal nanomaterial on the surface of another semiconductor or metal nanoparticle core is called capping. Semiconductor nanoparticles are coated with another semiconductor with a different band gap in a core-shell geometry to passivate the surface of the initial nanoparticle and enhance its emissive properties. While the mechanism of charge separation in a capped semiconductor system is similar to that in coupled semiconductor systems, interfacial charge transfer and charge collection in this multicomponent semiconductor system are significantly different. In coupled semiconductor systems, the two particles are in contact with each other and both holes and electrons are accessible for selective oxidation and reduction processes on different particle surfaces. On the other hand, capped semiconductors have a core-shell geometry. By depositing a relatively thick shell of the second semiconductor with a thickness is similar to the core radius it is possible to maintain the individual identities of the two semiconductors. Under these circumstances, only one of the charge carriers is accessible at the surface, while opposite charge transfer to the inner semiconductor occurs, thus improving the selectivity of the interfacial transfer and enhancing the oxidation or reduction reaction [126] (Figure 9). Core-shell geometry has an important consequence in terms of imparting enhanced photoelectrochemical stability to the system, taking into account that many of these semiconductors (especially group II–VI compounds) are prone to anodic photocorrosion in aqueous media [127].

Matijevic and coworker [128] prepared spherical ZnO particles coated with uniform layers of TiO$_2$. Such a capping process provides an economical way to deposit expensive semiconductor material on an inexpensive support and is convenient for building tandem semiconductor structures. Bedja and Kamat [129] prepared TiO$_2$-capped SnO$_2$ and SiO$_2$ colloids. The TiO$_2$-capped SnO$_2$ particles were 80－100 Å in diameter and exhibited improved photochromic and photocatalytic efficiencies compared with TiO$_2$-capped
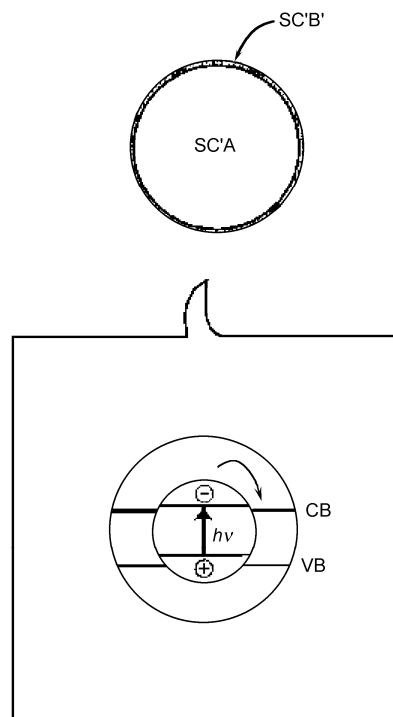

Figure 9   Electron transfer in a core-shell geometry [126].

SiO$_2$, TiO$_2$, SiO$_2$, and SnO$_2$ samples. The improved charge separation in this system was confirmed from the enhanced efficiency of hole trapping monitored by the absorption peak at 360 nm. The capped semiconductor system was useful for the oxidation of I$^-$ and SCN$^-$ and the quantum efficiency for I$^-$ oxidation was improved by a factor of 2–3 upon capping SnO$_2$ with TiO$_2$. Lim et al. [130] synthesized monodisperse silica/TiO$_2$ core-shell photocatalysts of varying thickness *via* a sol-gel route and measured their photocatalytic activity using the decolorization of methylene blue. The photocatalytic activity was greatest for the thickest shells but did not correlate precisely with specific surface area. Elder et al. [131] synthesized TiO$_2$/MoO$_3$ core-shell nanocrystalline materials. The photoabsorption energy of this system systematically shifted from 2.88 to 2.60 eV as the size of the composite nanoparticle was tuned from 80 to 40 Å. However, these materials showed a lower efficiency than Degussa P25 for the photocatalytic oxidation of acetaldehyde. Sung et al. [132] reported anatase/rutile core-shell structured TiO$_2$ particles synthesized by controlled heat treatment of poly(ethylene oxide)-TiO$_2$ hybrid particles. The mechanism of core-shell structure formation was based upon volume shrinkage, thermal expansion coefficient differences and further decomposition of organic components. These core-shell particles showed enhanced rates of photodecomposition compared with spherical and other commercially available particles, most probably because of the increased surface area of the nanoporous, nanocrystalline structure of the anatase core.

A new series of photocatalysts has been designed by

capping noble metal particles of Ag, Au, or Pt [133] with a semiconductor shell. Metal particles with a favorable Fermi level (0.4 V) such as silver and gold are good electron acceptors and facilitate rapid electron transfer from excited TiO_2. The transfer of electrons from the excited semiconductor to the metal is an important aspect that dictates the overall energetics and hence the efficiency of photocatalytic reduction. Hirakawa et al. [134] reported that Ag core/TiO_2 shell clusters were able to store electrons under UV irradiation and discharge them on demand in the dark. When these clusters were subjected to UV irradiation, a blue shift in the plasmon absorption band from 480 to 420 nm was observed, which reflects an increased electron density in the Ag core during photoirradiation.

Various research groups have studied TiO_2 capped with organic molecules. The photocatalytic investigation of TiO_2 nanocrystals capped with different organic molecules have been performed. The photocatalytic activity of oleic acid-TiO_2 nanocrystals was shown to be even higher than that of Degussa P25 [135]. This behavior indicates a direct involvement of the interface of the materials in photocatalytic reactions. Fittipaldi et al. [136] carried out multifrequency electron paramagnetic resonance studies on TiO_2 nanocrystals capped with organic moieties prepared by both nonhydrolytic and hydrolytic procedures. The presence of paramagnetic species (carbon radicals) on the surface of the TiO_2 nanocrystals was suggested to account for the high catalytic efficiency of such a nanostructured material.

12   Applications

12.1   Photoinduced hydrophilic coatings and self-cleaning devices

The deposition of dirt, soot, vehicular exhaust and other particulates results in the necessity of cleaning the surfaces of buildings. The growth of organisms, such as bacteria, algae and fungi disfigures the facades of buildings and results in mechanical weakening and eventual destruction. To prevent this, buildings can be coated with a layer of photocatalyst. Photocatalysis occurs in the presence of light with the energy corresponding to the band gap energy of the photocatalyst and causes the coating to chemically break down the organic particles adsorbed on the surface of the photocatalyst. Also, contact angle of water is increased, making the surface superhydrophobic which would allow dirt to be washed away easily [137].

The general concept of the self-cleaning capacity of TiO_2 is well known and the application of TiO_2 coatings to buildings for self-cleaning purposes is of considerable interest [138]. If a TiO_2 film is prepared with a certain percentage of SiO_2, it acquires superhydrophilic properties after UV illumination. In this case, electrons and holes are still produced but they react in a different way than normal photocatalysts. The electrons tend to reduce the Ti(IV)

cations to Ti(III), and the holes oxidize the O^{2-} anions. In this process, oxygen atoms are ejected, creating oxygen vacancies. Water molecules can then occupy these oxygen vacancies, producing adsorbed OH groups that tend to make the surface hydrophilic. The longer the surface is irradiated with UV light, the smaller the contact angle of water becomes. After about 30 min under a UV light source of moderate intensity, the contact angle approaches zero, meaning that water has a tendency to spread perfectly across the surface [12]. Toma et al. [139] reported the degradation of gaseous nitrogen oxide pollutants like NO and NO_x by sprayed TiO_2 coatings (around 52% for NO and 34% for NO_x).

Sekiguchi et al. [140] made TiO_2-coated silicone catheters for clean intermittent catheterization. They examined the photocatalytic antibacterial effect using light energy and the safety of this type of catheter for practical clinical use. These catheters were easily sterilized under sunlight. The survival rate of *Escherichia coli*, *Staphylococcus aureus*, *Pseudomonas aeruginosa* and *Serratia marcescens* in the liquid inside the TiO_2 catheter decreased to a negligible level within 60 min of exposure to UV irradiation.

12.2   Wastewater treatment

Over the last two decades, photocatalysis with TiO_2 nanoparticles has been shown useful for the degradation of wastewater pollutants. This process has several advantages including complete mineralization of organic pollutants like aliphatics, aromatics, polymers, dyes, surfactants, pesticides and herbicides to CO_2, water and mineral acids, no waste solids to dispose of and mild temperature and pressure conditions. Photocatalysis with TiO_2 nanoparticles uses two kinds of reaction systems, namely suspension and immobilized systems [141]. TiO_2 powders have higher photocatalytic efficiency than a coating because of their higher specific surface area. However, the separation of powder from the liquid state used in water treatment and recycling processes is troublesome because of the formation of aggregates, and also the depth of penetration of UV light is limited because of strong absorption by both catalyst particles and dissolved organic species. These difficulties can be overcome and the application of TiO_2 nanoparticles can also be expanded by employing various materials as substrates [139]. Glass beads or fiberglass mesh structures may increase the surface area available for catalysis. Taoda [142] developed photocatalytic silica gel by coating a transparent film of TiO_2 on beads of silica gel. Because the reaction area was large, it allowed highly efficient decomposition of harmful organic substances, unpleasant odors and colored matters present in wastewater.

In recent years, several review articles [51,78] have been published on photocatalytic water treatment with generally positive results, indicating the potential of photocatalytic oxidation technologies for neutralizing very diverse categories of toxic compounds in water. The photocatalytic degradation of phenol has been extensively studied because of

its high toxicity and ubiquity [36,143]. Bui et al. [144] completely mineralized two azo dyes, Reactive Red 4 (Cibacron Brilliant Red 3B-A) and Reactive Black 5 (Remazol Black B) to determine the potential of photocatalysis for the treatment of water using TiO$_2$ powder.

Prairie et al. [145] treated water contaminated with metal and organic species with TiO$_2$. They concluded that Ag(I), Cr(VI), Hg(II), and Pt(II) were easily treated by photocatalytic reduction with 0.1 wt% TiO$_2$, whereas Cd(II), Cu(II), and Ni(II) were not removed. The ability of TiO$_2$ to remove metals was found to depend on the standard reduction potential of the metal. Asmussen et al. [146] reported wastewater remediation using bifunctional electrodes that performed both photocatalytic degradation and electrochemical oxidation. A thin film of TiO$_2$ was coated on one side of a Ti plate, while an electrocatalyst (thin film of Ta$_2$O$_5$-IrO$_2$) was coated on the other side. These bifunctional electrodes exhibited superb activity for the degradation of common persistent toxic pollutants (4-nitrophenol and 2-nitrophenol) in industrial and agricultural wastewater. Mahmoodi et al. [141] studied the photocatalytic degradation of a textile dye (Acid Blue 25) in a photocatalytic reactor containing immobilized TiO$_2$ nanoparticles at pilot scale and showed that immobilized TiO$_2$ nanophotocatalysis was capable of degradation of Acid Blue 25 in textile wastewater, reducing its toxicity.

12.3 Degradation of pesticides

Pesticides (herbicides, insecticides, and fungicides) have a wide variety of structures and have been developed to exhibit an intended efficacy to specific pests, fungal diseases and weeds. Pesticides are usually applied as formulations to such targets in the field, and are considered cumulative and toxic. Their presence as contaminants in aquatic environments may cause serious problems for human beings and other organisms. The use of TiO$_2$ for environmental cleanup of organic pollutants through photooxidation has received much attention in the past decade. Various reports have been made on the degradation of pesticides using TiO$_2$ or modified TiO$_2$ in solution, as listed in Table 2 [147–153].

12.4 Production of hydrogen fuel

H$_2$ has great potential as a source of energy from the aspects of environmental preservation and energy security to realize a sustainable society in the future. For this purpose, H$_2$ should be produced from renewable resources and natural energy sources. Photocatalysis using solar energy has been widely studied as a possible system to produce hydrogen from water ever since the Honda-Fujishima effect was first reported in 1972 [3]. The possibility of solar photoelectrolysis was demonstrated for the first time with a system in which an n-type TiO$_2$ semiconductor electrode was connected through an electrical load to a platinum black counter electrode [154]. When the surface of the TiO$_2$ electrode was irradiated with near-UV light, photocurrent flowed from the platinum counter electrode to the TiO$_2$ electrode through the external circuit, showing that water can be decomposed into

Table 2 Degradation of pesticides using TiO$_2$ or modified TiO$_2$ in solution

No.	Pesticide	Chemical name	Category	Reference
1	Malathion	2-(dimethoxyphosphinothioylthio) butanedioic acid diethyl ester	organophosphorus insecticide	[147]
2	Methamidophos	(O,S-dimethyl phosphoramidothioate)	organophosphorus pesticides (insecticide-acaricide)	[148]
3	chlorfenapyr	4-bromo-2-(4-chlorophenyl)-1-ethoxymethyl-5-(trifluoromethyl)pyrrole-3-carbonitrile.	pyrrole group of pesticides (insecticide-miticide)	[149]
4	Phoxim	*N*-Diethoxyphosphinothioyloxybenzenecarboximidoyl cyanide	organophosphate insecticide	[150]
5	Dichlofenthion	O-(2,4-dichlorophenyl)O,O-diethyl phosphorothioate	insecticide	[151]
6	Bromophos ethyl	O-4-bromo-2,5-dichlorophenyl O,O-diethyl phosporothioate	insecticide	[151]
7	Bromophos methyl	O-4-bromo-2,5-dichlorophenyl O,O-dimethyl phosporothioate	insecticide	[151]
8	Parathion ethyl	O,O-diethyl O-4-nitrophenyl phosphorothiate	organophosphorus insecticide	[151]
9	Parathion methyl	O,O-dimethyl O-4-nitrophenyl phosphorothiate	organophosphorus insecticide	[151]
10	Atrazine	2-chloro-4-ethylamino-6-isopropylamino-1,3,5-triazine	herbicide	[151]
11	Cyanazine	2-chloro-4-(1-cyano-1-methylethylamino)-6ethylamino-1,3,5-triazine	herbicide	[151]
12	Irgarol	2-(methylthio)-4-(*tert*-butylamino)-6-(cyclopropylamino)-striazine	herbicide	[151]
13	Prometryne	2,4-bis(isopropylamino)-6-methylthio-1,3,5-triazine	herbicide	[151]
14	Propazine	2-chloro-4,6-bis(isopropylamino)-1,3,5-triazine	herbicide	[151]
15	Chlorotoluron	3-(3-chloro-4-methylphenyl)-1,1-dimethylurea,1	herbicide/ herbicide derivative	[152]
16	Metobromuron	3-(4-bromophenyl)-1-methoxy-1-methylurea	herbicide	[152]
17	Isoproturon	3-(4-isopropylphenyl)-1,1-dimethylurea	herbicide	[152]
18	Cinosulfuron	1-(4,6-dimethoxy-1,3,5-triazin-2-yl)-3-[2-(2-methoxyethoxy)phenylsulfonyl]urea	herbicide	[153]
19	Triasulfuron	1-[2-(2-chloroethoxy)phenylsulfonyl]-3-(4-methoxy-6-methyl-1,3,5-triazin-2-yl)urea	herbicide	[153]

oxygen and hydrogen without the application of an external voltage. The direction of the current revealed that oxygen evolution occurred at the TiO_2 electrode and hydrogen evolution occurred at the Pt electrode. Fujihara et al. [155] reported the photochemical splitting of water by combining two photocatalytic reactions on suspended TiO_2 particles, namely, the reduction of water to hydrogen using bromide ions, which were oxidized to bromine and the oxidation of water to oxygen using Fe^{3+} ions, which were reduced to Fe^{2+}. These two reactions were carried out in separate compartments and combined *via* platinum electrodes and cation-exchange membranes. At the electrodes, Fe^{2+} ions were oxidized by bromine and protons were transported through the membranes to maintain the electric neutrality and pH of the solutions in the two compartments. As a result, water was continuously split into hydrogen and oxygen under photoirradiation. The problem of back reactions was largely prevented because the concentrations of the products in solution were maintained at a low level. Kawai et al. [156] showed that TiO_2-assisted H_2 production could be significantly enhanced (56 times) by using a methanol/water mixture instead of water alone.

Seger and Kamat [157] constructed a polymer membrane electrode assembly consisting of a TiO_2 photoanode, Pt cathode, and proton exchange membrane to generate hydrogen continuously under UV excitation with no applied bias. Acidified methanol was oxidized at the UV-irradiated TiO_2 photocatalyst and H^+ ions were driven to the Pt cathode surface through the Nafion membrane. A generated photocurrent of 0.34 mA/cm^2 under UV irradiation showed effective operation of the fuel cell in reverse for solar hydrogen production. Yoshida et al. [158] examined the photocatalytic reaction of CH_4 gas with H_2O vapor over Pt/TiO_2 at room temperature and obtained H_2 and CO_2 as the main products with trace amounts of C_2H_6 and CO. Arakawa and Sayama found that Na_2CO_3 improved water splitting significantly when it was added to a Pt/TiO_2 suspension [159] and many other photocatalyst systems.

13   Conclusions

Semiconductor photocatalysis involves the formation of electron-hole pairs, which is initiated by band gap excitation of the semiconductor particle. Photocatalysis appears to be promising as a route for selective synthetic transformations or as an advanced oxidation process for environmental cleanup such as air purification, water disinfection, and hazardous waste remediation. Over the past few decades, continuous breakthroughs in the synthesis and modification of TiO_2 have realized new properties and applications with improved performance, starting from water photoelectrolysis (Honda-Fujishima effect) in the early 1970s to photocatalytic H_2 production in the 1980s, and photocatalysis and hydrophilicity of TiO_2 films in the 1990s. This steady progress has demonstrated that TiO_2 is playing and will continue to play an important role in the protection of the environment and in the search for renewable and clean energy technologies.

In this paper, an overview of the properties, modification and selected applications of TiO_2 as well as its future prospects is presented. Some of the major problems associated with photocatalysis are rapid charge recombination and back reaction and an inability to use visible light efficiently. Addition of electron donors can enhance photocatalytic activity by irreversibly reacting with valence band holes to prevent charge recombination. Doping of TiO_2 can inhibit charge recombination and expand its photoresponse to the visible region through the formation of impurity energy levels. Dye sensitization and coupling of semiconductors can also expand the light response of TiO_2 to the visible region. Excited dyes and small band gap semiconductors can inject electrons into the conduction of large band gap semiconductors, resulting in efficient charge separation and high photocatalytic efficiency. Selected applications of TiO_2 have been reviewed, including degradation of pesticides, photoinduced hydrophilic coatings and self-cleaning devices and production of hydrogen fuel.

Novel applications and industrial use of TiO_2 are anticipated for the future because of its low cost, photostability in solution, nontoxicity, redox selectivity and strong oxidizing power of holes. Continuous efforts to improve the photocatalytic properties of TiO_2 by surface modification will allow the full potential of this photocatalyst to be realized.

1   Kato S, Masuo F. Titanium dioxide-photocatalyzed oxidation. I. Titanium dioxide-photocatalyzed liquid phase oxidation of tetralin. Kogyo Kagaku Zasshi, 1964, 67: 42–50

2   McLintock S, Ritchie M. Reactions on titanium dioxide; photoadsorption and oxidation of ethylene and propylene. Trans Faraday Soc, 1965, 61: 1007–1016

3   Fujishima A, Honda K. Electrochemical photolysis of water at a semiconductor electrode. Nature, 1972, 238: 37–38

4   Frank S N, Bard A J. Heterogeneous photocatalytic oxidation of cyanide ion in aqueous solutions at titanium dioxide powder. J Am Chem Soc, 1977, 99: 303–304

5   Schrauzer G N, Guth T D. Photocatalytic reactions. 1. Photolysis of water and photoreduction of nitrogen on titanium dioxide. J Am Chem Soc, 1977, 99: 7189–7193

6   Schrauzer G N, Strampach N, Hui L N. Nitrogen photoreduction on desert sands under sterile conditions. Proc Natl Acad Sci USA, 1983, 80: 3873–3876

7   Kreutler B, Bard A J. Heterogenous photocatalytic preparation of supported catalyst. Photodeposition of platinum on titanium dioxide powder and other substrates. J Am Chem Soc, 1978, 100: 4317–4318

8   Hsiao C Y, Lee C L, Ollis D F. Heterogenous photocatalysis: Degradation of dilute solution of dichloromethane (CH_2Cl_2), chloroform ($CHCl_3$), and carbon tetrachloride (CCl_4) with illuminated TiO_2 photocatalyst. J Catal, 1983, 82: 418–423

9   Matsunaga T, Tomato R, Nakajima T, et al. Photoelectrochemical

sterilization of microbial cells by semiconductor powders. FEMS Microbiol Lett, 1985, 29: 211–214

10 Fujishima A, Ohtsuki J, Yamashita T, et al. Behavior of tumor cells on photoexcited semiconductor surface. Photomed Photobiol, 1986, 8: 45–46

11 Regan O, Grätzel M. A low-cost, high-efficiency solar cell based on dye-sensitized colloidal TiO₂ film. Nature, 1991, 353: 737–740

12 Fujishima A, Rao T N, Tryk D A. Titanium dioxide photocatalysis. J Photochem Photobiol C Photochem Rev, 2000, 1: 1–21

13 Wang R, Hashimoto K, Fujishima A, et al. Light-induced amphiphilic surfaces. Nature, 1997, 388: 431–432

14 Watson S, Beydoun D, Amal R. Synthesis of a novel magnetic photocatalyst by direct deposition of nanosized TiO₂ crystals onto a magnetic core. J Photochem Photobiol A Chemistry, 2002, 148: 303–311

15 Sonawane R S, Kale B B, Dongare M K. Preparation and photo-catalytic activity of Fe-TiO₂ thin films prepared by sol-gel dip coating. Mater Chem Phys, 2004, 85: 52–57

16 Sreethawong T, Suzuki Y, Yoshikawa S. Synthesis, characterization, and photocatalytic activity for hydrogen evolution of nanocrystalline mesoporous titania prepared by surfactant-assisted templating sol-gel process. J Solid State Chem, 2005, 178: 329–338

17 Diamandescu L, Vasiliu F, Tarabasanu-Mihaila D, et al. Structural and photocatalytic properties of iron- and europium-doped TiO₂ nanoparticles obtained under hydrothermal conditions. Mater Chem Phys, 2008, 112: 146–153

18 Lai T Y, Lee W C. Killing of cancer cell line by photoexcitation of folic acid-modified titanium dioxidenanoparticles. J Photochem Photobiol A Chem, 2009, 204: 148–153

19 Mizukoshi Y, Ohtsu N, Semboshi S, et al. Visible light responses of sulfur-doped rutile titanium dioxide photocatalysts fabricated by anodic oxidation. App Cat B Environ, 2009, 91: 152–156

20 Wang C, Ao Y, Wang P, et al. A facile method for the preparation of titania-coated magnetic porous silica and its photocatalytic activity under UV or visible light. Colloid Surf A: Physicochem Eng Aspects, 2010, 360: 184–189

21 Kaewgun S, Lee B I. Deactivation and regeneration of visible light active brookite titania in photocatalytic degradation of organic dye. J Photochem Photobiol A: Chem, 2010, 210: 162–167

22 Rocha O R, Dantas R F, Duarte M M M B, et al. Oil sludge treatment by photocatalysis applying black and white light. Chem Eng J, 2010, 157: 80–85

23 Carp O, Huisman C L, Reller A. Photoinduced reactivity of titanium dioxide. Prog in Solid State Chem, 2004, 32: 33–117

24 Mor G K, Varghese O K, Paulose M, et al. A review on highly ordered, vertically oriented TiO₂ nanotube arrays: Fabrication, material properties, and solar energy applications. Solar Energ Mater Solar Cell, 2006, 90: 2011–2075

25 Chen X, Mao S S. Titanium dioxide nanomaterials: Synthesis, properties, modifications, and applications. Chem Rev, 2007, 107: 2891–2959

26 Thompson T L, Yates Jr J T. Surface science studies of the photoactivation of TiO₂-New photochemical processes. Chem Rev, 2006, 106: 4428–4453

27 Diebold U. The surface science of titanium dioxide. Sur Sci Rep, 2003, 48: 53–229

28 Linsebigler A L, Lu G, Yates J T. Photocatalysis on TiO₂ surfaces: Principles, mechanisms, and selected results. Chem Rev, 1995, 95: 735–758

29 Simons P Y, Dachille F. The structure of TiO₂ II, a high-pressure phase of TiO₂. Acta Cryst, 1967, 23: 334–336

30 Latroche M, Brohan L, Marchand R, et al. New hollandite oxides: TiO₂(H) and K₀.₀₆TiO₂. J Solid State Chem, 1989, 81: 78–82

31 Cromer D T, Herrington K. The structures of anatase and rutile. J Am Chem Soc, 1955, 77: 4708–4709

32 Baur V W H. Atomabstände und bindungswinkel im brookit, TiO₂. Acta Crystallogr, 1961, 14: 214–216

33 Mo S, Ching W. Electronic and optical properties of three phases of titanium dioxide: Rutile, anatase and brookite. Phys Rev B, 1995, 51: 13023–13032

34 Norotsky A, Jamieson J C, Kleppa O J. Enthalpy of transformation of a high pressure polymorph of titanium dioxide to the rutile modification. Science, 1967, 158: 338–389

35 Zhang Q, Gao L, Guo J. Effects of calcination on the photocatalytic properties of nanosized TiO₂ powders prepared by TiCl₄ hydrolysis. Appl Catal B Environ, 2000, 26: 207–215

36 Sclafani A, Palmisano L, Schiavello M. Influence of the preparation methods of titanium dioxide on the photocatalytic degradation of phenol in aqueous dispersion. J Phys Chem, 1990, 94: 829–832

37 Muscat J, Swamy V, Harrison N M. First-principles calculations of the phase stability of TiO₂. Phy Rev B, 2002, 65: 1–15

38 Tanaka K, Capule M F V, Hisanaga T. Effect of crystallinity of TiO₂ on its photocatalytic action. Chem Phys Lett, 1991, 187: 73–76

39 Selloni A. Anatase shows its reactive side. Nature Mater, 2008, 7: 613–615

40 Yang H G, Sun C H, Qiao S Z, et al. Anatase TiO₂ single crystals with a large percentage of reactive facets. Nature, 2008, 453: 638–641

41 Wunderlich W, Oekermann T, Miao L, et al. Electronic properties of nano-porous TiO₂-and ZnO-thin films-comparison of simulations and experiments. J Ceram Process Res, 2004, 5: 343–354

42 Paxton A T, Thiên-Nga L. Electronic structure of reduced titanium dioxide. Phys Rev B, 1998, 57: 1579–1584

43 Banerjee S, Gopal J, Muraleedharan P, et al. Physics and chemistry of photocatalytic titanium dioxide: Visualization of bactericidal activity using atomic force microscopy. Current Sci, 2006, 90: 1378–1383

44 Li G, Chen L, Graham M E, et al. A comparison of mixed phase titania photocatalysts prepared by physical and chemical methods: The importance of the solid-solid interface. J Mol Catal A Chem, 2007, 275: 30–35

45 You X, Chen F, Zhang J. Effects of calcination on the physical and photocatalytic properties of TiO₂ powders prepared by sol-gel template method. J Sol-Gel Sci Tech, 2005, 34: 181–187

46 Hu Y, Tsai H L, Huang C L. Phase transformation of precipitated TiO₂ nanoparticles. Mater Sci Eng A, 2003, 344: 209–214

47 Wang J, Li R H, Zhang Z H, et al. Heat treatment of nanometer anatase powder and its photocatalytic activity for degradation of acid red B dye under visible light irradiation. Inorg Mater, 2008, 44: 608–614

48 Ohtani B, Ogawa Y, Nishimoto S. Photocatalytic activity of amorphous-anatase mixture of Titanium(IV) oxide particles suspended in aqueous solutions. J Phys Chem B, 1993, 101: 3746–3752

49 Yu J, Zhao X, Zhao Q. Photocatalytic activity of nanometer TiO₂ thin films prepared by the sol-gel method. Mater Chem Phys, 2001, 69: 25–29

50 Han H, Ba R. Buoyant photocatalyst with greatly enhanced visible-light activity prepared through a low temperature hydrothermal method. Ind Eng Chem Res, 2009, 48: 2891–2898

51 Hoffmann M R, Martin S T, Choi W, et al. Environmental applications of semiconductor photocatalysis. Chem Rev, 1995, 95: 69–96

52 Marcus R A. Reorganization free energy for electron transfers at liquid-liquid and dielectric semiconductor-liquid interfaces. J Phys Chem, 1990, 94: 1050–1055

53 Mills A, Hunte A J. An overview of semiconductor photocatalysis. J Photochem Photobiol A Chem, 1997, 108: 1–35

54 Dawson G, Chen W, Zhang T, et al. A study on the effect of starting material phase on the production of trititanate nanotubes. Solid State Sci, 2010, 12: 2170–2176

55 Yana J, Fenga S, Lua H, et al. Alcohol induced liquid-phase synthesis of rutile titania nanotubes. Mat Sci Eng B, 2010, 172: 114–120

56 Mozia S. Application of temperature modified titanate nanotubes for removal of an azo dye from water in a hybrid photocatalysis-MD process. Catalysis Today, 2010, 156: 198–207

57 Pradhan S K, Reucroft P J, Yang F, et al. Growth of TiO₂ nanorods by metalorganic chemical vapor deposition. J Crystal Growth, 2003, 256: 83–88

58 Limmer S J, Chou T P, Cao G Z. A study on the growth of TiO₂ nanorods using sol electrophoresis. J Mat Sci, 2004, 39: 895–901

59 Attar A S, Ghamsari M S, Hajiesmaeilbaigi F, et al. Synthesis and characterization of anatase and rutile TiO₂ nanorods by tem-

plate-assisted method. J Mat Sci, 2008, 43: 5924–5929

60   Hagfeldtt A, Grätzel M. Light-induced redox reactions in nanocrystalline systems. Chem Rev, 1995, 95: 49–68

61   Bahnemann D W, Kormann C, Hoffmann M R. Preparation and characterization of quantum size zinc oxide: A detailed spectroscopic study. J Phys Chem, 1987, 91: 3789–3798

62   Sivula K, Formal F L, Grätzel M. WO_3-Fe_2O_3 Photoanodes for water splitting: A host scaffold, guest absorber approach. Chem Mater, 2009, 21: 2862–2867

63   Miller R J D, McLendon G L, Nozik A J, et al. Surface Electron-transfer Processes. New York: VCH, 1995

64   Nishikiori H, Qian W, El-Sayed M A, et al. Change in titania structure from amorphousness to crystalline increasing photoinduced electron-transfer rate in dye-titania system. J Phys Chem C Lett, 2007, 111: 9008–9011

65   Benkö G, Skårman B, Wallenberg R, et al. Particle size and crystallinity dependent electron injection in fluorescein 27-sensitized TiO_2 films. J Phys Chem B, 2003, 107: 1370–1375

66   Li X Z, Zhao W, Zhao J C. Visible light-sensitized semiconductor photocatalytic degradation of 2,4-dichlorophenol. Sci China Ser B-Chem, 2002, 45: 421–425

67   Hirano K, Suzuki E, Ishikawa A. Sensitization of TiO_2 particles by dyes to achieve H_2 evolution by visible light. J Photochem Photobiol A Chem, 2000, 136: 157–161

68   Kay A, Grätzel M. Low cost photovoltaic modules based on dye sensitized nanocrystalline titanium dioxide and carbon powder. Sol Energy Mater Sol Cells, 1996, 44: 99–117

69   Grätzel M. Dye-sensitized solar cells. J Photochem Photobiol C Photochem Rev, 2003, 4: 145–153

70   Wu T, Lin T, Zhao J, et al. TiO_2-assisted photodegradation of dyes. 9. Photooxidation of a squarylium cyanine dye in aqueous dispersions under visible light irradiation. Environ Sci Technol, 1999, 33: 1379–1387

71   Burda C, Lou Y, Chen X, et al. Enhanced nitrogen doping in TiO_2 nanoparticles. Nano Lett, 2003, 3: 1049–1051

72   Szaciłowski K, Macyk W, Drzewiecka-Matuszek A, et al. Bioinorganic photochemistry: Frontiers and mechanisms. Chem Rev, 2005, 105: 2647–2694

73   Grätzel M, Howe R F. Electron paramagnetic resonance studies of doped TiO_2 colloids. J Phys Chem, 1990, 94: 2566–2572

74   Choi Y, Termin A, Hoffmann M R. The role of metal ion dopants in quantum-sized TiO_2: Correlation between photoreactivity and charge carrier recombination dynamics. J Phys Chem, 1994, 98: 13669–13679

75   Joshi M M, Labhsetwar N K, Mangrulkar P A, et al. Visible light induced photoreduction of methyl orange by N-doped mesoporous titania. App Catal A General, 2009, 357: 26–33

76   Maruska H P, Ghosh A K. Transition-metal dopants for extending the response of titanate photoelectrolysis anodes. Sol Energy Mater, 1979, 1: 237–247

77   Gautron J, Lemasson P, Marucco J M. Correlation between the non-stoichiometry of titanium dioxide and its photoelectrochemical behaviour. Faraday Discuss Chem Soc, 1981, 70: 81–91

78   Fox M A, Dulay M T. Heterogeneous photocatalysis. Chem Rev, 1995, 93: 341–357

79   Xin B, Ren Z, Wang P, et al. Study on the mechanisms of photoinduced carriers separation and recombination for Fe^{3+}-TiO_2 photocatalysts. App Surf Sci, 2007, 253: 4390–4395

80   Li R, Chen W, Wang W. Magnetoswitchable controlled photocatalytic system using ferromagnetic Fe-doped titania nanorods photocatalysts with enhanced photoactivity. Sep Purif Technol, 2009, 66: 171–176

81   Periyasami V, Chinnathambi M, Chinnathambi S, et al. Photocatalytic activity of iron doped nanocrystalline titania for the oxidative degradation of 2,4,6-trichlorophenol. Catal Today, 2009, 141: 220–224

82   Khan M A, Han D H, Yang O B. Enhanced photoresponse towards visible light in Ru doped titania nanotube. Appl Surf Sci, 2009, 255: 3687–3690

83   Prasad G K, Singh B, Ganesan K, et al. Modified titania nanotubes

for decontamination of sulphur mustard. J Hazard Mater, 2009, 167: 1192–1197

84   El-Bahy Z M, Ismail A A, Mohamed R M. Enhancement of titania by doping rare earth for photodegradation of organic dye (Direct blue). J Hazard Mater, 2009, 166: 138–143

85   Wang C, Ao Y, Wang P, et al. Photocatalytic performance of Gd ion modified titania porous hollow spheres under visible light. Mat Lett, 2010, 64: 1003–1006

86   Wang C, Ao Y, Wang P, et al. Preparation, characterization, photocatalytic properties of titania hollow sphere doped with cerium. J Hazard Mater, 2010, 178: 517–521

87   Rupa A V, Divakar D, Sivakumar T. Titania and noble metals deposited titania catalysts in the photodegradation of tartrazine. Catal Lett, 2009, 132: 259–267

88   Papp J, Shen H S, Kershaw R, et al. Titanium(IV) oxide photocatalysts with palladium. Chem Mater, 1993, 5: 284–288

89   Thampi K R, Kiwi J, Grätzel M. Methanation and photomethanation of carbon dioxide at room temperature and atmospheric pressure. Nature, 1987, 327: 506–508

90   Adachi K, Ohta K, Mizuno T. Photocatalytic reduction of carbon dioxide to hydrocarbon using copper-loaded titanium dioxide. Sol Energ, 1994, 53: 187–190

91   Wong W K, Malati M A. Doped TiO_2 for solar energy applications. Sol Energy, 1986, 36: 163–168

92   Wu N L, Lee M S. Enhanced TiO_2 photocatalysis by Cu in hydrogen production from aqueous methanol solution. Inter J Hydro Energ, 2004, 29: 1601–1605

93   Turner M, Golovko V B, Vaughan O P H, et al. Selective oxidation with dioxygen by gold nanoparticle catalysts derived from 55-atom clusters. Nature, 2008, 454: 981–983

94   Sakthivel S, Shankar M V, Palanichamy M, et al. Enhancement of photocatalytic activity by metal deposition: Characterization and photonic efficiency of Pt, Au and Pd deposited on TiO_2 catalyst. Water Res, 2004, 38: 3001–3008

95   Xu J, AoY, Chen M, et al. Low-temperature preparation of Boron-doped titania by hydrothermal method and its photocatalytic activity. J Alloy Comp, 2009, 484: 73–79

96   Xu J, Ao Y, Chen M. Preparation of B-doped titania hollow sphere and its photocatalytic activity under visible light. Mat Lett, 2009, 63: 2442–2444

97   Asahi R, Morikawa T, Ohwaki T, et al. Visible-light photocatalysis in nitrogen-doped titanium oxides. Science, 293: 269–271

98   Diwald O, Thompson T L, Goralski E G, et al. The effect of nitrogen ion implantation on the photoactivity of Ti_{O2} rutile single crystals. J Phys Chem B, 2004, 108: 52–57

99   Ao Y, Xu J, Zhang S, et al. A one-pot method to prepare N-doped titania hollow spheres with high photocatalytic activity under visible light. Appl Surf Sci, 2010, 256: 2754–2758

100 Dong L, Cao G X, Ma Y, et al. Enhanced photocatalytic degradation properties of nitrogen-doped titania nanotube arrays. Trans Nonferrous Met Soc China, 2009, 19: 1583–1587

101 Yu J C, Yu J G, Ho W K, et al. Effects of F⁻ doping on the photocatalytic activity and microstructures of nanocrystalline TiO_2 powder. Chem Mater, 2002, 14: 3808–3816

102 Sakthivel S, Kisch H. Daylight photocatalysis by carbon-modified titanium dioxide. Angrew Chem Int Ed, 2003, 42: 4908–4911

103 Park J H, Kim S, Bard A J. Novel carbon-doped TiO_2 nanotube arrays with high aspect ratios for efficient solar water splitting. Nano Lett, 2006, 6: 24–28

104 Meng N, Leung M K H, Leung D Y C, et al. A review and recent developments in photocatalytic water-splitting using TiO_2 for hydrogen production. Renew Sust Energ Rev, 2007 11: 401–425

105 Yang P, Lu C, Hua N, et al. Titanium dioxide nanoparticles co-doped with Fe^{3+} and Eu^{3+} ions for photocatalysis. Mater Lett, 2002, 57: 794–801

106 Vasiliu F, Diamandescu L, Macovei D, et al. Fe-and Eu-doped TiO_2 photocatalytical materials prepared by high energy ball milling. Top Catal, 2009, 52: 544–556

107 Song K, Zhou J, Bao J, et al. Photocatalytic activity of (copper, ni-

trogen)-codoped titanium dioxide nanoparticles. J Am Ceram Soc, 2008, 91: 1369–1371

108   Xu J, Ao Y, Fu D. A novel Ce, C-codoped TiO₂ nanoparticles and its photocatalytic activity under visible light. Appl Surf Sci, 2009, 256: 884–888

109   Shen X Z, Liu Z C, Xie S M, et al. Degradation of nitrobenzene using titania photocatalyst co-doped with nitrogen and cerium under visible light illumination. J Hazard Mater, 2009, 162: 1193–1198

110   Yang X, Ma F, Li K, et al. Mixed phase titania nanocomposite codoped with metallic silver and vanadium oxide: New efficient photocatalyst for dye degradation. J Hazard Materer, 2010, 175: 429–438

111   Vogel R, Hoyer P, Weller H. Quantum-sized PbS, CdS, Ag₂S, Sb₂S₃, and Bi₂S₃ particles as sensitizers for various nanoporous wide-bandgap semiconductors. J Phys Chem, 1994, 98: 3183–3188

112   Gopidas K R, Bohorquez M, Kamat P V. Photophysical and photochemical aspects of coupled semiconductors: charge-transfer processes in colloidal cadmium sulfide-titania and cadmium sulfide-silver(I) iodide systems. J Phys Chem, 1990, 94: 6435–6440

113   Nayak B B, Acharya H N, Mitra G B, et al. Structural characterization of Bi₂₋ₓSbₓS₃ films prepared by the dip-dry method. Thin Solid Film, 1983, 105: 17–24

114   Bessekhouad Y, Robert D, Weber J V. Bi₂S₃/TiO₂ and CdS/TiO₂ heterojunctions as an available configuration for photocatalytic degradation of organic pollutant. J Photochem Photobiol A Chem, 2004, 163: 569–580

115   Song K Y, Park M K, Kwon Y T, et al. Preparation of transparent particulate MoO₃/TiO₂ and WO₃/TiO₂ films and their photocatalytic properties. Chem Mater, 2001, 13: 2349–2355

116   Grandcolas M, Du K L, Louvet F B A, et al. Porogen template assisted TiO₂ rutile coupled nanomaterials for improved visible and solar light photocatalytic applications. Catal Lett, 2008, 123: 65–71

117   Wang C, Shao C, Zhang X, et al. SnO₂ Nanostructures-TiO₂ nanofibers heterostructures: Controlled fabrication and high photocatalytic properties. Inorg Chem, 2009, 48: 7261–7268

118   Vinodgopal K, Bedja I, Kamat P V. Nanostructured semiconductor films for photocatalysis. Photoelectrochemical behavior of SnO₂/TiO₂ composite systems and its role in photocatalytic degradation of a textile azo dye. Chem Mater, 1996, 8: 2180–2187

119   Zhang L W, Fu H B, Zhu Y F. Efficient TiO₂ photocatalysts from surface hybridization of TiO₂ particles with graphite-like carbon. Adv Funct Mater, 2008, 18: 2180–2189

120   Zhang L W, Wang Y, Xu T, et al. Surface hybridization effect of C60 molecules on TiO₂ and enhancement of the photocatalytic activity. J Mol Cataly A: Chem, 2010, 331: 7–14

121   Ji S, Murakami S, Kamitakahara M, et al. Fabrication of titania/hydroxyapatite composite granules for photo-catalyst. Mater Res Bull, 2009, 44: 768–774

122   Takeuchi M, Sakai S, Ebrahimi A, et al. Application of highly functional Ti-oxide-based photocatalysts in clean technologies. Top Cataly, 2009, 52: 1651–659

123   Zhang X, Lei L, Zhang J, et al. A novel CdS/S-TiO₂ nanotubes photocatalyst with high visible light activity. Separ Purif Tech, 2009, 66: 417–421

124   Ferry J L, Glaze W H. Photocatalytic reduction of nitroorganics over illuminated titanium dioxide: Electron transfer between excited-state TiO₂ and nitroaromatics. J Phys Chem B, 1998, 102: 2239–2244

125   Kumar A, Jain A K. Photophysics and photochemistry of colloidal CdS-TiO₂ coupled semiconductors-photocatalytic oxidation of indole. J Mol Catal A Chemical, 2001, 165: 265–273

126   Rajeshwar K, de Tacconi N R, Chenthamarakshan C R. Semiconductor-based composite materials: Preparation, properties, and performance. Chem Mater, 2001, 13: 2765–2782

127   Gerischer H. On the stability of semiconductor electrodes against photodecomposition. J Electroanal Chem, 1977, 82: 133–143

128   Ocana M, Hsu W P, Matijevic E. Preparation and properties of uniform-coated colloidal particles. 6. Titania on zinc oxide. Langmuir, 1991, 7: 2911–2916

129   Bedja I, Kamat P V. Capped semiconductor colloids. Synthesis and

photoelectrochemical behavior of TiO₂ capped SnO₂ nanocrystallites. J Phys Chem, 1995, 99: 9182–9188

130   Lim S H, Phonthammachai N, Pramana S S, et al. Simple route to monodispersed silica-titania core-shell photocatalysts. Langmuir, 2008, 24: 6226–6231

131   Elder S H, Cot F M, Su Y, et al. The discovery and study of nanocrystalline TiO₂-(MoO₃) core-shell materials. J Am Chem Soc, 2000, 122: 5138–6146

132   Sung Y M, Lee J K, Chae W S. Controlled crystallization of nanoporous and core/shell structure titania photocatalyst particles. Crystal Growth Desig, 2006, 6: 805–808

133   Liz-Marzan L M, Mulvaney P. The assembly of coated nanocrystals. J Phys Chem B, 2003, 107: 7312–7326

134   Hirakawa T, Kamat P V. Electron storage and surface plasmon modulation in Ag@TiO₂ clusters. Langmuir, 2004, 20: 5645–5647

135   Comparelli R, Fanizza E, Curri M L, et al. Photocatalytic degradation of azo dyes by organic-capped anatase TiO₂ nanocrystals immobilized onto substrates. Appl Catal B, 2005, 55: 81–91

136   Fittipaldi M, Curri M L, Comparelli R, et al. A multifrequency EPR study on organic-capped anatase TiO₂ nanocrystals. J Phys Chem C, 2009, 113: 6221–6226

137   Parkin I P, Palgrave R G. Self-cleaning coatings. J Mater Chem, 2005, 15: 1689–1695

138   Mills A, Hodgen S, Lee S K. Self-cleaning titania films: An overview of direct, lateral and remote photo-oxidation processes. Res Chem Intermed, 2005, 31: 295–308

139   Toma F L, Bertrand G, Klein D, et al. Development of photocatalytic active TiO₂ surfaces by thermal spraying of nanopowders. J Nanomater, 2008, 1–8

140   Sekiguchi Y, Yao Y, Ohko Y, et al. Self-sterilizing catheters with titanium dioxide photocatalyst thin films for clean intermittent catheterization: Basis and study of clinical use. Int J Urology, 2007, 14, 426–430

141   Mahmoodi N M, Arami M. Degradation and toxicity reduction of textile wastewater using immobilized titania nanophotocatalysis. J Photochem Photobiol B Biol, 2009, 94: 20–24

142   Taoda H. Development of TiO₂ photocatalysts suitable for practical use and their applications in environmental cleanup. Res Chem Intermed, 2008, 34: 417–426

143   Matthews R W, Mc Evoy S R. Photocatalytic degradation of phenol in the presence of near-UV illuminated titanium dioxide. J Photochem Photobiol A Chem, 1992, 64: 231–246

144   Bui T H, Karkmaz M, Puzenat E, et al. Solar purification and potabilization of water containing dyes. Res Chem Intermed, 2007, 33: 421–431

145   Prairie M R, Evans L R, Martinez S L. Destruction of organics and removal of heavy metals in water via TiO₂, photocatalysis in chemical oxidation: Technology for the nineties. In: Second International Symposium. Lancaster: Technomic Publishing Company, 1994

146   Asmussen R M, Tian M, Chen A. A new approach to wastewater remediation based on bifunctional electrodes. Environ Sci Technol, 2009, 43: 5100–5105

147   Ali R, Hassan S H. Degradation studies on paraquat and malathion using TiO₂/ZnO based photocatalyst. Malaysian J Anal Sci, 2008, 12: 77–87

148   Dai K, Peng T, Chen H, et al. Photocatalytic degradation and mineralization of commercial methamidophos in aqueous titania suspension. Environ Sci Technol, 2008, 42: 1505–1510

149   Cao Y, Yi L, Huang L, et al. Mechanism and pathways of chlorfenapyr photocatalytic degradation in aqueous suspension of TiO₂. Environ Sci Technol, 2006, 40: 3373–3377

150   Dai K, Peng T, Chen H, et al. Photocatalytic degradation and mineralization of commercial methamidophos in aqueous titania suspension. Environ Sci Technol, 2009, 43: 1540–1545

151   Konstantinou I K, Sakellarides T M, Sakkas V A, et al. Photocatalytic degradation of selected s-triazine herbicides and organophosphorus insecticides over aqueous TiO₂ suspensions. Environ Sci Technol, 2001, 35: 398–405

152   Parra S, Olivero J, Pulgarin C. Relationships between physicochemical

properties and photoreactivity of four biorecalcitrant phenylurea herbicides in aqueous TiO$_2$ suspension. Appl Catal B, 2002, 36: 75–85

153 Vulliet E, Emmelin C, Chovelon J M, et al. Photocatalytic degradation of sulfonylurea herbicides in aqueous TiO$_2$. Appl Catal B, 2002, 38: 127–137

154 Fujishima A, Kobayakawa K, Honda K. Hydrogen production under sunlight with an electrochemical photocell. J Electrochem Soc, 1975, 122: 1487–1489

155 Fujihara K, Ohno T, Matsumura M. Splitting of water by electrochemical combination of two photocatalytic reactions on TiO$_2$ particles. J Chem Soc Faraday Trans, 1998, 94: 3705–3709

156 Kawai M, Naito S, Tamaru K, et al. The mechanism of photocatalytic

hydrogen production from gaseous methanol and water: IR spectroscopic approach. Chem Phys Lett, 1983, 98: 377–380

157 Seger B, Kamat P V. Fuel cell geared in reverse: Photocatalytic hydrogen production using a TiO$_2$/nafion/Pt membrane assembly with no applied bias. J Phys Chem C, 2009, 113: 18946–18952

158 Yoshida H, Hirao K, Nishimoto J, et al. Hydrogen production from methane and water on platinum loaded titanium oxide photocatalysts. J Phys Chem C, 2008, 112: 5542–5551

159 Sayama K, Arakawa H. Significant effect of carbonate addition on stoichiometric photodecomposition of liquid water into hydrogen and oxygen from platinum-titanium(IV) oxide suspension. J Chem Soc Chem Commun, 1992, 150–152